Computer Methods and Programs in Biomedicine 209 (2021) 106301

Contents lists available at ScienceDirect

Computer Methods and Programs in Biomedicine

journal homepage: www.elsevier.com/locate/cmpb

A review of mathematical model-based scenario analysis and interventions for COVID-19☆

Regina Padmanabhan[a], Hadeel S. Abed[a], Nader Meskin[a,*], Tamer Khattab[a], Mujahed Shraim[b], Mohammed Abdulla Al-Hitmi[a]

[a] Department of Electrical Engineering, Qatar University, Qatar
[b] Department of Public Health, College of Health Sciences, QU Health, Qatar University, Qatar

ARTICLE INFO

Article history:
Received 25 February 2021
Accepted 17 July 2021

Keywords:
COVID-19
Mathematical models
Active control
Unified framework

ABSTRACT

Mathematical model-based analysis has proven its potential as a critical tool in the battle against COVID-19 by enabling better understanding of the disease transmission dynamics, deeper analysis of the cost-effectiveness of various scenarios, and more accurate forecast of the trends with and without interventions. However, due to the outpouring of information and disparity between reported mathematical models, there exists a need for a more concise and unified discussion pertaining to the mathematical modeling of COVID-19 to overcome related skepticism. Towards this goal, this paper presents a review of mathematical model-based scenario analysis and interventions for COVID-19 with the main objectives of (1) including a brief overview of the existing reviews on mathematical models, (2) providing an integrated framework to unify models, (3) investigating various mitigation strategies and model parameters that reflect the effect of interventions, (4) discussing different mathematical models used to conduct scenario-based analysis, and (5) surveying active control methods used to combat COVID-19.

1. Introduction

COVID-19 infection that started in December 2019 has spread over wide geographic areas. Until now there is a sustained transmission in several countries across the globe. The experience of epidemiologists and scientists in dealing with past pandemics such as Spanish flu, zika virus, cholera, HIV, ebola, etc. has helped the government to quickly take control measures including border closures, lockdown, isolation of infected patients, and frequent disinfection of contaminated surfaces, to face this unprecedented social, economic, and health emergency. To accelerate the mitigation process, several state-of-the-art technologies, including (1) next-generation gene sequencing to identify the pathogen, (2) artificial intelligence-based algorithms to classify infected or noninfected cases, (3) mathematical model-based analysis to characterize disease transmission dynamics, and (4) big-data techniques to track the mobility of the population or to identify transmission hotspots have been used [47,55,89,123,126,134]. In particular, mathematical models are used to characterize various phases of disease transmission in a population and to optimize expenditure related to interventions and hospital facility management.

Traditional and social media has also done their part in raising awareness and supporting people worldwide with the necessary information and guidelines from policymakers [29,133]. Media has advocated the importance of bringing down R_0, the basic reproduction number below 1, and discussed the forecast, results, and implications of research and model-based studies related to COVID-19. The extend of transmission and the threat posed by this virus can be assessed based on the reproduction number R_0, with R_0 close to 2.5 up to 60% of the world population (4.68 billion) can get infected [92]. With various interventions in place, the effective reproduction number (R_e) in different parts of the world is 0.88–1.25 bringing down the global confirmed cases and deaths as of February 2021 to 109 and 2.39 million, respectively [1–3]. However, with R_e, close to 1.25, up to 16.67% of the world population (1.3 billion) can get infected. This implies that we are yet to hit a stable endemic period and nowhere close to complete containment which is necessary to restore social freedom and economic recovery. Even though initially, this virus was thought of as respiratory pneumonia, now it is clear that it can additionally affect other or-

☆ This publication was made possible by QU emergency grant no. QUERG-CENG-2020-2 from Qatar University. Open Access funding provided by the Qatar National Library. The statements made herein are solely the responsibility of the authors.

* Corresponding author.
E-mail addresses: regina.ajith@qu.edu.qa (R. Padmanabhan), ha1513750@student.qu.edu.qa (H.S. Abed), nader.meskin@qu.edu.qa (N. Meskin), tkhattab@ieee.org (T. Khattab), mshraim@qu.edu.qa (M. Shraim), m.a.alhitmi@qu.edu.qa (M.A. Al-Hitmi).

https://doi.org/10.1016/j.cmpb.2021.106301

gans such as the brain, kidney, and heart [54]. Moreover, an extensive infection is unaffordable due to limited hospital capacity and the threat of associated mortalities. Hence, continued social distancing, limited interactions/gatherings, isolation of infected, and rapid deployment of vaccines are warranted across the globe until containment is achieved [34,92].

Coming to the epidemiological factors that lead to the COVID-19 pandemic, as reported in Li et al. [71], using SEIR-model-based analysis it is estimated that 86% of infections that happened in China before Jan 23, 2020, were undocumented. Even though the percentage of unreported cases were reduced by implementing rapid and random testing strategies, a significant proportion of infected have gone undetected. Living one year with the pandemic, it is clear that the hidden asymptomatic patients are the main culprits that overthrow the containment efforts taken by various countries and the reason behind re-emergence of the disease once restrictions are lifted [38,59]. Cluster busting approach has substantiated the occurrence of asymptomatic and presymptomatic disease transmission [38]. Another relevant disease statistics is that superspreaders who constitute 10–20% of the total population are responsible for most (80%) of the transmission in a society [38]. Individuals with considerable viral load (viral shed) and/or increased contact rate are included in the superspreaders category [17]. Identifying unreported infections or hidden asymptomatic transmission nodes is quite important as it facilitates the effective implementation of containment strategies. Evidently, spreading awareness about the disease and mass testing has played a critical role in the containment of the disease or in approaching a stable endemic region in some countries such as Singapore, Australia, New Zealand, and Qatar [15,74,108,122]. As reflected in the values of R_0 and R_e, intervention response data from various countries show that restrictions such as lockdown, border closures, social distancing, and decisions to lift/relax restrictions have a significant impact on the progression of the epidemic [125].

Mathematical models have been extensively used during the past and present pandemics to have a closer look at the disease spreading dynamics and to foresee when and at what cost the disease will be contained [88,90,110,132]. In general, modeling approaches include deterministic models, stochastic models, and their combinations which are built and validated using population data in a region or metapopulation data with inter-region mobility details. Few models have analyzed the virus/carrier dynamics inside the human body [32,36,49,65,70,101] and some have investigated the effect of preventive vaccine and the use of supporting curative drugs if any [24,42,67,91]. Mathematical modeling is one of the important tools in our arsenal against COVID-19 and it is indeed important to consolidate existing research in this area and point out challenges and research gaps. Hence, in Section 2 of this paper, we discuss existing reviews on mathematical modeling of COVID-19 to enable better positioning of the value added by this review. Next in Section 3, we present a general model and highlight the parameters affected by various interventions. Section 4 presents scenario-specific models and discusses critical assessments based on such models. In Section 5, we discuss the use of control-theoretic methods to derive active intervention protocols to mitigate COVID-19 followed by discussions and conclusions in Sections 6 and 7.

2. Existing relevant reviews

Most of the existing papers present a review on the important epidemiological features such as transmissibility, series interval, disease severity, case fatality, and types of intervention strategies [23,38,63,68,72,83,85,97,130]. The general outcomes expected out of mathematical model-based analysis are to (1) know the expected number of cases within a time frame, (2) evaluate outcomes of possible interventions, (3) know conditions for the existence of disease-free equilibrium, (4) derive control inputs when the resources are limited, and (5) know the optimal time frame to achieve a cost-effective outcome. In the case of an ongoing pandemic, often there will be a lack of data for model building and validation. Depending upon the important population parameters that affect the epidemics, there can be very complex models. However, fitting such complex models with available data may be difficult. On the other hand, using a simpler model will compromise accuracy. Hence, there will be a trade-off between data availability and the complexity/accuracy of the model. Deterministic compartmental models are the most widely used mathematical models for investigating the dynamics of epidemics. Logistic models have also been used [51,75,123].

Table 1 summarises the existing reviews on mathematical modeling of COVID-19. In [89], based on the review of 61 articles, the authors point out that SEIR and SIR models are the most widely used for prediction and CNN-based deep learning methods are the most used method for classification of X-ray and CT-scans related to COVID-19 diagnosis. A comprehensive review of various deterministic and stochastic modeling approach highlighting the assumptions involved in building the models are provided in Tang et al. [123]. Lessons learned and conclusions derived in terms of various epidemiological, virological, and clinical characteristics are listed in Fang et al. [38]. A similar analysis using elementary SIR and SEIR models to evaluate epidemiological features (asymptomatic infections, herd immunity) and intervention strategies are reported in Wang et al. [130] and Lin et al. [72]. In [85], authors highlight the importance of mathematical modeling and also point out that considerable methodological issues arise in estimating even simple epidemiological quantities. Moreover, it is important to understand the extent of asymptomatic spread and duration of immunity after infection, and also to adapt models according to the context [84,85,114].

In [75], the exponential increase of disease transmission is estimated using simple SIR, SEIR, and logistic models. Specifically, a review of various multi-compartment models in estimating the initial exponential growth rate and R_0 is discussed. The SIR model provides a good fit to the initial exponential growth rate even though it ignores subpopulations in various epidemiological status. The logistic and Richards models give robust estimates when fitting windows up to the epidemic peak are used [75]. In [16], the SIR model based on the data from ECDC (European Centre for Disease Prevention and Control) for countries including Italy, Germany, Spain, UK is discussed. Model parameter estimation and intervention strategies are also explained for this SIR model. Evidence-based cost-effective analysis is summarised in Juneau et al. [56].

Identifying the importance of mathematical models, in Chen et al. [31] four challenges and non-uniformity or disparity in mathematical models are pointed out. Similarly, applications, potentials and limitation of mathematical model-based studies are highlighted in Wang [129]. In [129], fixed transmission rates, modeling limited to human-to-human, ignoring a decrease in transmission due to an increase in compliance are pointed out as a limitation. In [120], limitations of prediction models, and the importance of intelligent computing on symptom-based identification and analysis of COVID-19 is reviewed. However, as shown in later parts of this review, many models have incorporated time-varying transmission rates, environmental transmission, and compliance of people in the model.

As shown in Table 1 some of the existing reviews point out the discrepancy and inconsistencies in models as a challenge that hinders their effective utilization in decision-making [31,129]. Specific issues that are pointed out are inconsistency in the definition of terms and inadequate incorporation of social and individual be-

Table 1
Existing reviews on mathematical modeling of COVID-19; CFR-case fatality ratio, AI-artificial intelligence.

Ref.	Model	Remark/conclusion
Mohamadou et al. [89]	General models	Overview of mathematical models, AI-based methods, and data sets pertaining to COVID-19. SEIR and SIR most used models.
Tang et al. [123]	SIR and SEIR, and general	Nationwide macromechanistic and community level micromodels are discussed highlighting the properties of the model, assumptions involved, and a comparison with stochastic/statistical approach based analysis is provided.
Fang et al. [38]	General models	Consolidated epidemiological, virological, and clinical facts. Estimated that 10–20% of infected population is responsible for 80% of transmission. Longer-range exposure/transmission can occur in closed and poorly-ventilated spaces.
Wang et al. [130]	SIR and SEIR	Evaluated epidemiological features: CFR = 4.5–5.1%, $R_0 = 2.2$–3.11, and discussed effects of herd immunity and interventions. More model-based studies are needed.
Lin et al. [72]	SEIR	Evaluated epidemiological features: CFR = 2.9%, $R_0 = 3.77$, $R_c = 1.88$, and $\tau_{in} = 5.9$.
Meehan [85]	SEIR	General discussion on CFR and R_0. Points out that mean $\tau_{in} = 3.6$–7.4 days, and there exists methodological difficulty in estimating parameters of even very simple models.
Ma [75]	SIR, SEIR, Logistic, and Richards	Compared applicability of four models to estimate initial growth rate and R_0. SIR model provides good estimate of growth rate.
Shah et al. [114]	General models	Critical review, pointed out that the influence of lockdown and adherence to social distancing should be modeled for specific countries.
McBryde et al. [84]	General models	There is a need to adapt epidemiological models and economic models to assist policy makers.
Barwolff [16]	SIR	Analysed lockdown and social distancing strategies. SIR model is insufficient to analyze all kinds of interventions.
Juneau et al. [56]	General models	Evidence-based cost-effective analysis is done. Contact tracing and case isolation are the most cost-effective intervention.
Chen et al. [31]	General models	Points out the non-uniformity or disparity in mathematical models and inadequate inclusion of social and individual behavior.
Wang [129]	General models	Discuss applications, limitations, and potentials of models.

haviors that influence the overall dynamics. In fact, even though there exist many mathematical models that already address the research gaps pointed out in Chen et al. [31] and Wang [129], all such models are not discussed in any review. Moreover, there does not exist any review that talks about various realistic scenarios related to COVID-19 under one heading. Hence, in this paper, (1) we define a general model and a set of common notations to unify compartmental models of COVID-19, (2) consolidate values of important epidemiological parameters, (3) discuss armaments for anti-epidemic battle and point out model parameters that are altered/affected by each intervention, (4) highlight importance of scenario-based studies using 12 mathematical models that incorporate specific compartments relevant to each scenario, and (5) review literature that use control theoretic approaches to derive active control solution for mitigating COVID-19. We also provide unified model equations (consistent notations) of all the 12 models (Scenarios A to L) discussed in this paper in a supplementary file. The integrated framework discussed allows easy classification of various populations, identification of parameters that influence the dynamics of each population, and comparison of existing compartmental models in the literature.

3. A generalized mathematical model for epidemic analysis

In this section, a general model that can be used to derive compartmental model equations for all the 11 scenario-based models that are discussed in later parts of this section is presented. Moreover, the range of values of important time-constants involved, inter-compartmental transmission rates, and specific model parameters that reflect the changes due to various interventions are discussed.

Model equations for a general model with n compartments as shown in Fig. 1 are given by:

$$\begin{aligned}\dot{x}_i(t) = &- \sum_{\substack{j=1,\dots,n,\\ i\neq j}} k_{ij}(t,\tau,x_m(t),u(t))x_i(t)\\ &+ \sum_{\substack{j=1,\dots,n,\\ i\neq j}} k_{ji}(t,\tau,x_m(t),u(t))x_j(t) - k_0(t,\tau,x_m(t),u(t))x_i(t)\\ &+ \rho(t,\tau,x_m(t),u(t)), \quad i=1,\dots,n \end{aligned} \tag{1}$$

where $x_i(t)$, $i = 1,\dots,n$, is the population in the i-th compartment, $k_{ij}(\cdot)$ denotes the inter-compartmental transition rates that models the population outflow from the ith compartment to jth compartment, $\rho(t,\tau,x_m(t),u(t))$ is the import of cases from other regions or from another subpopulation with different epidemic characteristics, τ is the time delay if any in inter-compartmental transitions, and $u(t)$ models the influence of control intervention on inter-compartmental transition rate(s).

In (1), except for the import of cases ($\rho(t,\tau,x_m(t),u(t))$), all outward arrows corresponds to the term

$$-\sum_{\substack{j=1,\dots,n,\\ i\neq j}} k_{ij}(t,\tau,x_m(t),u(t))x_i(t)$$

and inward arrows corresponds to the term

$$\sum_{\substack{j=1,\dots,n,\\ i\neq j}} k_{ji}(t,\tau,x_m(t),u(t))x_j(t),$$

where $x_i(t)$ and $x_j(t)$ are the compartments from which the arrows originate, and $x_m(t)$ is any other compartmental dynamics that influences the rate constant. It is apparent that an inter-compartmental transition rate can be influenced by the dynamics in a compartment which is not at the anterior or posterior end of the arrow. For instance, considering the simple SEIR model ($n = 4$) in Fig. 2, the transition of the susceptibles to the exposed compartment can be modeled as $\dot{S}(t) = -\beta(t)S(t)$, where $\beta(t) = \beta_0 I(t)$. As shown in Fig. 1 there can be removal ($k_0(t,\tau,x_m(t),u(t))$) from certain or all compartments due to natural or COVID-19 related death. In most models, birth and natural death are assumed to be at the same rate and hence only direct death due to COVID-19 and indirect natural death due to hospital saturation are included. Note that indirect natural death due to hospital saturation can be reduced by implementing various COVID-19 mitigation measures, hence $k_0(t,\tau,x_m(t),u(t))$ can be modeled in terms of $u(t)$. Here, $x_m(t)$ can be a compartment that accommodates hospitalized ($H(t)$) or/and severely infected ($I_s(t)$) patients.

Fig. 2 is a susceptible-exposed-infected-recovered (SEIR) model with the time constants and transmission rates pertaining to COVID-19. The incubation period is the time after exposure to the virus until symptom onset. The average incubation period is 5 to

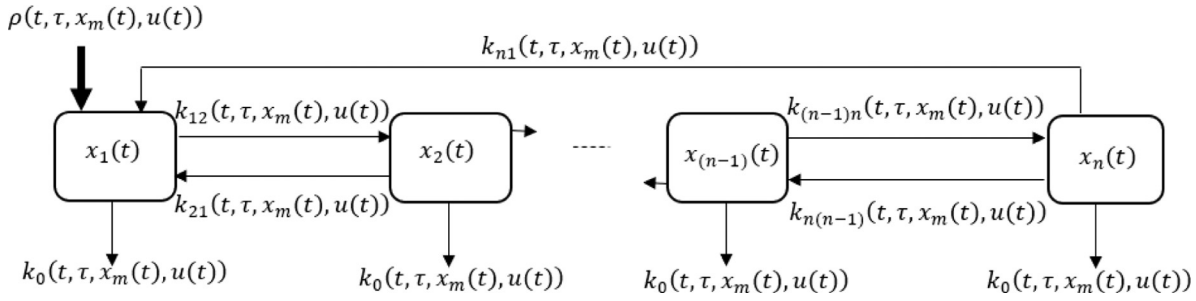

Fig. 1. Schematic diagram representing the general model given by (1). In this figure, the dark inward arrow denote the import of population from other region/subpopulation.

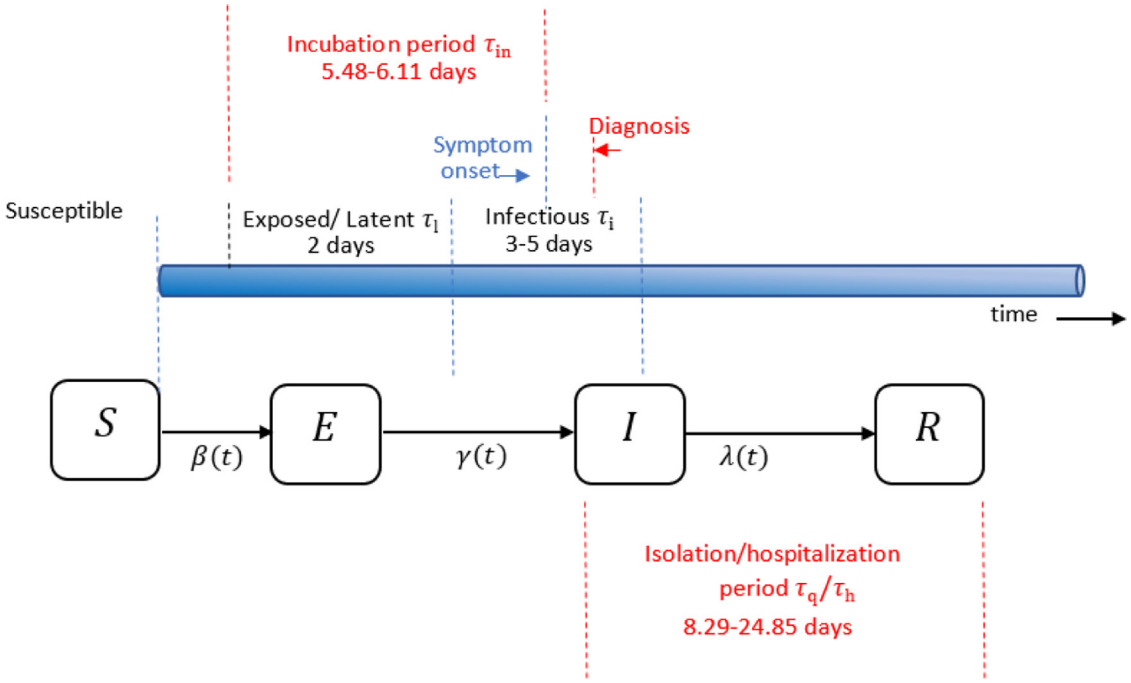

Fig. 2. Simple SEIR (susceptible-exposed-infected-recovered) model with time constants and inter-compartmental transmission rates [4,39,72,73].

6 days (up to 14 days), hence quarantine period is set as 1 to 2 weeks [4,39]. Similar to other viral infections, coronavirus is believed to weaken the interferon-dependent immune response initially, and hence symptoms are exhibited only after the latent period. The latent period (exposed period) is the duration for which an individual is exposed to a virus but not infectious yet [73]. As per the SEIR model-based analysis done in Liu et al. [73], Peng et al. [99], $1/\tau_l = 12\ h^{-1}$ which implies $\tau_l \approx 2$ days. Serial interval and the average time between symptom onset to diagnosis is estimated to be 5.06 and 5.82 days, respectively [39]. The infectious time duration, which was estimated to be $\tau_i = 9.94\ (3.9 - 13.5)$ in initial studies [72], was later reduced to $\tau_i = 3$–5 days [38]. Before the onset of symptoms, for around 1 to 2 days, the patients are most contagious. The delay between symptom onset and diagnosis may vary from 4 to 7 days and if not diagnosed and isolated within the infectious period, the transmission to others is high and on an average 39.04% (18.38–64.56%) of total transmission is estimated to be the presymptomatic transmission, as the chances of diagnosis are much less during the presymptomatic period, unless included in randomly tested group. Based on 17 studies that include 2304 patients, the asymptomatic transmission is estimated to be 5.58–14.18% [38,39].

The SEIR model with four compartments shown in Fig. 2 or its modified version are the most widely used compartmental model. Additional compartments are added to depict disease transmission dynamics of specific subpopulations (e.g. frontliners, children, etc.) or epidemiological status (infected, quarantined, etc.). Similar to Fig. 1 and model described by (1), the model equations for all the 12 models discussed in the coming sections of this paper can be easily written with respect to the transition rates marked in respective model diagrams. For instance, with respect to (1), the equation for second compartment in Fig. 2, can be written as $\dot{x}_2(t) = -k_{23}(t)x_2(t) + k_{12}(t)x_1(t)$, where $x_1(t) = S(t)$, $x_2(t) = E(t)$, $k_{23}(t) = \gamma(t)$, and $k_{12}(t) = \beta(t)$.

3.1. Armaments for anti-epidemic battle and associated model parameters

From the past experiences in dealing with earlier epidemics, the world looked at mathematical modeling as a reliable tool that can provide causal insights about the disease transmission dynamics. Model-based studies that analyzed disease-free equilibrium have concluded in the early March 2020 itself that unless vigorous control measures are taken, the world will see an extensive spread of COVID-19 [18,109,128]. It is quite apparent that vigorous and rapid strategic efforts were in place to curb the infection and mortalities related to COVID-19. The timelines of observatory procedures, disease diagnosis/testing, and clinical assistance are key factors that

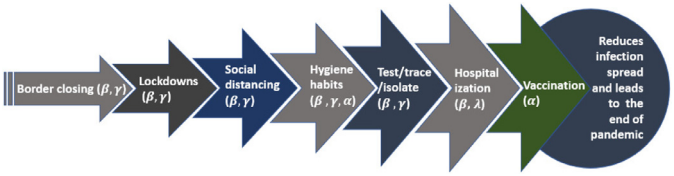

Fig. 3. Model parameters that are affected by various interventions are given in parenthesis. Border closure, lockdown, social distancing, hygiene habits, testing, contact tracing, and isolation reduce the exposure rate β and infection rate γ. Hygiene habits increase the protection rate α. Reverse quarantine of elderly and chronically ill population, compliance with regulations, and vaccination also increase protection rate α. Hospitalization and use of supportive medicines increase recovery rate λ. All the interventions together contribute to the journey towards the containment of the epidemics.

decide the overall outcome of pandemic containment efforts. The difference in the value of R_0 (2.5) and R_e (1.25) indicates the importance of various interventions in reducing the otherwise disastrous health, social, and economic impacts of COVID-19. Pharmaceutical interventions (PHI) including testing, isolation in hospitals, use of supportive drugs and critical care; and nonpharmaceutical interventions (NPIs) such as border closure, lockdown, contact tracing, home quarantine, restricted social interactions, and hygiene awareness campaigns are used worldwide.

The presence of hidden transmission nodes (asymptomatic patients) is the evident challenge that overturned and nullified the containment efforts. Mass testing strategies and early isolation play a critical role in identifying unreported infections due to mild or no symptoms. The test-trace-isolate strategy is the most effective NPI [38,68]. In the case of the primary or first identified infected person in a community, often isolation starts after the onset of symptoms, whereas for a person already in isolation due to contact with the primary infected person may start showing symptoms during the period of isolation which significantly reduces secondary transmissions (Fig. 2). In a study, it is pointed out that, 1-day reduction in the delay to isolate/quarantine an infected can substantially decrease total infection and mortality (by 68–80%). This points out the need to quickly isolate/quarantine infected individuals by implementing mass and random testing [116].

Apart from the exposure rate, β, infection rate, γ, and recovery rate, λ, marked in Fig. 2, some models use protection rate, α, to model the transition of an individual to a protected compartment due to reverse quarantine. Fig. 3 shows the model parameters that accommodate the influence of various PHIs and NPIs. Compared to all other interventions, cluster busting via intense and rapid contact tracing and isolation is the most cost-effective approach to reduce disease transmission throughout the timeline of a pandemic [68]. Notably, this approach is most cost-effective during the initial period or when implemented in an area where infections are not widespread. As the disease transmission progresses, the clusters become substantially wide and pose practical difficulty in effective implementation. In a model, the possibility of re-infection reflects as a decrease in the protection rate α and an increase in the exposure rate β. A time dependent loss of immunity can be modeled by incorporating a delay term in the movement of the population from the recovered compartment to the susceptible or infected compartment. An increase in infection due to social gathering or due to import of cases from other regions are modeled as a step-wise increase in β or γ.

4. Scenarios

In this section, we discuss mathematical models that can be used for scenario-based analysis at the community-level or nationwide. Table 2, 3 and 4 summarize the parameter notations used in this paper and Table 5 presents the mathematical models that represent various scenarios. Even though there are several variations of SIR and SEIR models, policy makers are looking for mathematical models that can be used to derive decisions pertaining to real time scenarios. Particularly, the influence of

- regional dynamics, inter-regional movement of infected cases, and import and export of cases,
- differential disease severity, recovery rates of detected and hospitalized cases,
- differential disease transmission among hospital staffs, other frontliners, the general public, white/blue collar workers, etc.,
- influence of concentration of virus on various surfaces,
- constraints including hospital saturation, availability of a vaccine, cost of interventions,
- school closing/opening influence of other hot spots,
- detected and undetected cases, and
- compliance of people, reverse quarantine of elderly/chronically ill, and protection by vaccination,

on the overall disease transmission dynamics are the scenarios discussed in this paper. In the following subsections, we discuss the models listed in Table 5. Figs. 4–15 show the models that are used for various scenario based-analysis. Model equations pertaining to

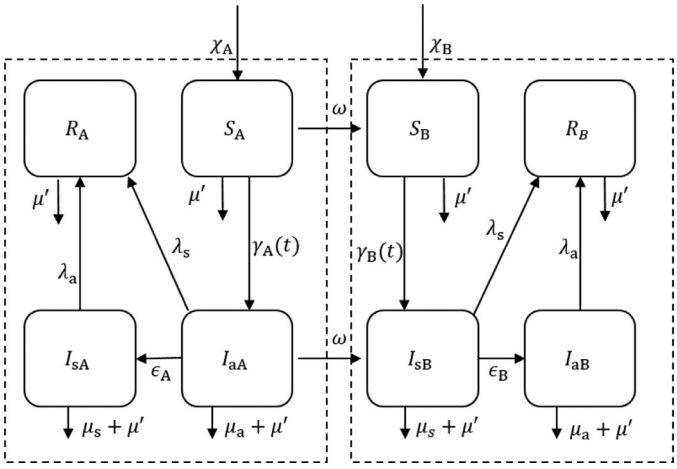

Fig. 4. Model 1: Mathematical model of COVID-19 that describes the mobility of individuals from severely infected region to mildly infected one. $N(0)_{A,B} = 8 \times 10^6$, $I_{sA}(0) = I_{aA}(0) = 2500$, $I_{sB}(0) = I_{aB}(0) = 250$, $R_{0A} = \frac{\gamma_A \chi_A}{(\mu'+\omega)(\mu_a+\mu'+\epsilon_A+\lambda_a+\omega)}$, and $R_{0B} = \frac{\gamma_B[\chi_B + \frac{\omega\chi_A}{\mu'+\omega}]}{\mu'(\mu_a+\mu'+\epsilon_B+\lambda_a)}$, $\lambda_a = 1/8$ (per unit time), $\lambda_s = 1/14$ (per unit time), $\omega_{max} = 0.4/(365 \times 8 \times 10^6)$, $\mu_s = 0.02/11$, $\mu_a = 0.2/11$ (per unit time), $\mu' = 0.007/365$ (per unit time), $\epsilon_i = \epsilon_0 + k_\epsilon r$, $\epsilon_0 = 1/11$, $k_\epsilon = 0.3$, and $\chi_i = 260$, $i = A, B$ (newborns per unit time) [50]. Control intervention $u_i(t)$ is assumed to alter $\gamma_i(t)$, where $\gamma_i(t) = \gamma_0(1-u_i(t))^2 S_i(t) I_i(t)$, $i = A, B$, and $\gamma_0 = 6.25 \times 10^{-8}$ (per unit time). .

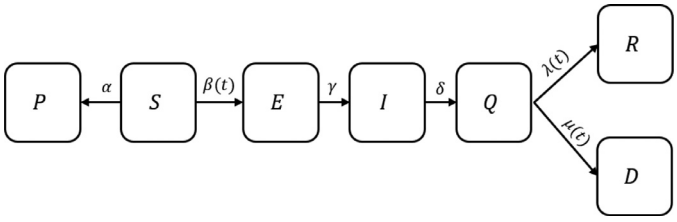

Fig. 5. Model 2: Mathematical model of COVID-19 to study the transmission of COVID-19 for 5 regions in China. $\beta_i(t) = \beta_{0i}\frac{I_i(t)}{N_i}$, $i = 1, \ldots, 5$, for Mainland, Hubei province, Wuhan, Beijing, and Shanghai, respectively, $N_1(0) = 1340 \times 10^6$, $N_2(0) = 45 \times 10^6$, $N_3(0) = 14 \times 10^6$, $N_4(0) = 22 \times 10^6$, $N_5(0) = 24 \times 10^6$, $E_1(0) = 696$, $E_2(0) = 592$, $E_3(0) = 318$, $E_4(0) = 27$, $E_5(0) = 18$, $I_1(0) = 652$, $I_2(0) = 515$, $I_3(0) = 389$, $I_4(0) = 19$, $I_5(0) = 23$, $\beta_{0i} = 1.0$ (1/day), $i = 1, 2, 3, 5$, $\beta_{04} = 0.99$ (1/day), $\tau_1 = \frac{1}{\gamma} = 2$ (days) for the 5 regions, $\tau_{qi} = \delta_i^{-1}$, $i = 1, 2, 3, 4, 5$, $\delta_1^{-1} = 6.6$ (days), $\delta_2^{-1} = 7.2$ (days), $\delta_3^{-1} = 7.4$ (days), $\delta_4^{-1} = 5.7$ (days), $\delta_5^{-1} = 5.6$ (days), $\alpha_1 = 0.172$ (1/day), $\alpha_2 = 0.133$ (1/day), $\alpha_3 = 0.085$ (1/day), $\alpha_4 = 0.175$ (1/day), $\alpha_5 = 0.183$ (1/day), and $R_0 = \beta \times \delta^{-1} \times (1-\alpha)^T$, where T is the number of days [99].

Table 2
Variable notations used for various subpopulations categorized according to epidemiological status .

Variable	Description
$S(t)$	Susceptible population
$S_c(t)$	Complaint/educated susceptible
$S_f(t)$, $S_g(t)$	Frontliners and general population
$P(t)$	Protected population
$V(t)$	Vaccinated population
$E(t)$	Exposed population
$I(t)$	Infected population
$I_{am}(t), I_{as}(t)$	Asymptomatic population which later move to mildly or severely infected compartments
$I_m(t), I_s(t)$	Mildly and severely infected population
$I_f(t), I_g(t)$	Infected frontliners or general public
$I_{au}(t), I_{ad}(t)$	Infected asymptomatic undetected and detected cases
$I_u(t), I_d(t)$	Infected symptomatic undetected and detected cases
$C(t)$	Virus concentration in the environment
$Q(t)$	Quarantined population
$H(t)$	Population isolated or moved to hospital
$R(t)$	Recovered population
$D(t)$	Dead population
$\Lambda_M(t)$	Information matrix
$X(t)$	Cumulative incidence
$Z(t)$	Mean-zero stochastic drift
$W(t)$	Workplace mobility
$\Pi(t)$	Regression coefficient

Table 3
Parameter notations.

Parameter	Description
β	Exposure/transmission rate
β_v	Rate at which uninfected cells gets infected with virus
γ	Infection rate or force of infection
δ, δ_a	Quarantine rate, quarantine rate for asymptomatic cases
α	Insusceptible/protection rate
ϵ	Test rate
ψ, ψ_q	Hospitalization rate, hospitalization rate after quarantine
$\lambda, \lambda', \lambda_q$	Recovery rate, recovery rate from ICU, from hospital isolation
μ	COVID-19 related death rate
μ'	Natural death rate
σ	Reinfection or loss of immunity
ω	Mobility rate
d	Rate of virus decay in the environment
ρ	Import of cases
Γ	Recruitment rate
ν	S_c to S transition rate
ζ	S to S_c transition due to dissemination of disease information
ξ	Transition rate between I_s and I_{sc}
e	Behavioral change, inflection point?, or association rate
a, b, f, f', θ	Proportion of one population that transit to other
γ'	Asymptomatic but infectious to symptomatic infected
m	Modification parameter that changes the transmission/infection rate
m_e, m_q, m_h	Modification factors for exposed, quarantined, and hospitalized individuals
m_a, m_s	Modification factor for asymptomatic and symptomatic cases
m_{ac}, m_{sc}	Modification factor for contained asymptomatic and symptomatic cases
p	Proportion of mild infections
R_0	Basic reproduction number
d	Virus decay rate
C_{50}	The concentration of virus on a surface/environment that is related to 50% of possibility for an individual to get infected
β_{ch}	Transmission from contaminated surface to human
γ_0	Threshold of infectivity that induce behavioral change in a population
γ_{va}, γ_{vs}	Viral shedding rate of asymptomatic and symptomatic patients to the environment
γ'	Rate transfer of asymptomatic to the symptomatic/sick class
λ_a, λ_s	Recovery rate for asymptomatic and symptomatic cases
λ_{au}, λ_u	Recovery rate for undetected asymptomatic and symptomatic cases
ϕ	Probability at which contact causes infection
$\gamma_{au}, \gamma_{ad}, \gamma_u, \gamma_d$,	Infection rate of asymptomatic-undetected, asymptomatic-detected, symptomatic-undetected, symptomatic-detected,

these models can be written using the generalized form proposed in (1) with respect to the general model in Fig. 1. The initial conditions and model parameter values (units) are also given in Figs. 4–15. See supplementary file for model equations of all the models discussed in this paper.

4.1. Scenario: inter-regional disease transmission

Mathematical models can be used to analyze nationwide or community level disease transmission and to study the influence of the inter-regional movement of cases on the overall disease

Table 4
Parameter notations, cont'd.

Parameter	Parameter description
τ_{in}, τ_l, τ_a, τ_s, τ_i, τ_q, τ_h	Mean incubation, latency, asymptomatic, symptomatic, infectious, quarantine, and hospital stay time
χ	Number of newborns in a population
k_ϵ	Sensitivity coefficient
r	Amount of allocated resources
μ_a, μ_s, μ_h	Death rate of asymptomatic, symptomatic, and hospitalized patients
φ	Rate of vaccination
φ_0	Information-based vaccination rate
$1-\varphi_1$	Maximum vaccination coverage due to information
η	Relative susceptibility of vaccinated
Ω	Reduced susceptibility due to previous infection
Λ_t	Inverse of time delay related to information
Λ_c	Information coverage
Ω_0	Relative susceptibility of recovered
η_0	Relative susceptibility of vaccinated
M	Michaelis-Menten parameter related to information-based vaccination
κ	Exponential rate of increase in disease transmission
K	Saturation in disease transmission
u	Intervention
δ'	Q to S transition rate
r_v	Rate of release of infectious viral particles
s	Reduction in susceptibility due to vaccination/immunization
Δ_{ad}, Δ_d	Diagnosis/detection rate of asymptomatic and symptomatic patients
Δ_{uu}, Δ_{dd}	Rate of symptom onset in asymptomatic undetected and asymptomatic detected patients
Δ_s, Δ_{ds}	Rate at which symptomatic infected individuals who are undetected and detected move to severely ill category
$\varkappa$	Population density
ϖ	Proportion of elderly population

Table 5
Mathematical models that discuss real time scenarios.

Model no.	Features	Scenario(s) [ref]
1. Fig. 4	Extended SIR model for 2 regions. Accounted for mobility and limited resource availability.	Resource constraint, duration of restriction, and influence of human mobility across regions [50].
2. Fig. 5	Parameters for 5 regions.	Protection by NPI intervention [99].
3. Fig. 6	Conducted intervention analysis.	Differential disease severity, indirect death due to saturated hospitals [34].
4. Fig. 7	Parameters from previous findings. Conducted sensitivity analysis.	Differential dynamics of frontliners and general public, import of cases [22].
5. Fig. 8	Estimated parameters and validated model using data. Conducted equilibrium point analysis.	Influence of viral shed on surfaces and educated /compliant population, reinfection, rate of asymptomatic to symptomatic [59].
6. Fig. 9	Investigated positivity and well posedness of problem.	Contained, noncontained, quarantine, and intensive care compartments. Model for social behavior of complaint population [64].
7. Fig. 10	Used Pontryagins minimum principle to derive optimal NPI interventions.	Influence of public health education, quarantine, and hospitalization [76].
8. Fig. 11	Parameter estimated and investigated lockdown implementation and relaxing scenario in NJ.	Age and social interaction data at home, work, and school [41].
9. Fig. 12	Accounted for delay.	Influence of school re-opening delay [62].
10. Fig. 13	Modified SIR model with detected and undetected case delineation to re-estimate CFR. Re-estimated model parameters according to 6 stages of interventions.	Influence of mass testing [43].
11. Fig. 14	Influence of media coverage.	Protection of subpopulation by vaccination [24].
12 Fig. 15	Virus dynamics.	Can be used to analyze virus dynamics under drug/vaccine administration [49].

transmission trend. Such investigations are imperative to make decisions pertaining to lockdowns, border closures, and suspension of international travel. In [50], an extended SIR model is used to model inter-regional movement between region A and B. Fig. 4 shows the model discussed in Hu et al. [50]. As shown in Fig. 4, ω is used to model the mobility rate, and as ω increases the reproduction number of region B (R_{0B}) increases. Also, note that the influence of lockdown in regions A and B on the respective infection rates are modeled in $\gamma_i(t)$. Similarly, in Kucharski et al. [65], international travel from Wuhan is modeled using a stochastic transmission model. According to the inter-region mobility based analysis, it is concluded that the travel control is effective in bringing down R_0 from 2.35 (95% CI 1.15–4.77) on Jan 23 to 1.05 (0.41–2.39) that is 1 week after imposing travel restriction.

4.2. Scenario: protected subpopulation

Another scenario of interest is to know the impact of implementing reverse quarantine (protecting from infection) of the elderly population or people with chronic illness. In this case, an additional compartment ($P(t)$) can be added to model the dynamics of the protected subpopulation as shown in Fig. 5. Based on the analysis using the seven compartment model depicted in Fig. 5, and the epidemic data from 5 regions in China (Mainland, Hubei province, Wuhan, Beijing, and Shanghai), it is shown that the average contact rate is significantly different in different regions [99]. This study also reveals a positive correlation between infection rate (γ) and mean quarantine period (δ^{-1}) and a negative correlation between γ and protection rate (α) thus highlighting the importance of increased self-protection, disinfection, and early quaran-

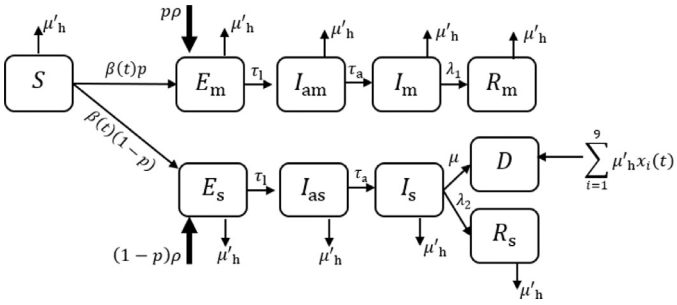

Fig. 6. Model 3: Mathematical model of COVID-19 that accounts for disease severity and hospital saturation, where $N(0) = 67 \times 10^6$, $I(0) = 120$, $S(0) = N(0) - I(0) = 66.99 \times 10^6$, $I_{m0} = pI_0$, $I_{s0} = (1-p)I_0$, $E_m(0) = E_s(0) = I_{am}(0) = I_{as}(0) = R_m(0) = R_s(0) = D(0) = 0$, $R_0 = 2.5$, $\mu'_h = 0$, if $I_s(t) < H$, $\mu'_h = \mu_h$, if $I_s(t) \geq H$, $\mu = \mu_{min}$, if $I_s(t) < H$, $\mu = \mu_{max}$ if $I_s(t) \geq H$, $\mu_{min} = 8.82 \times 10^{-3}$ (1/day), $\mu_{max} = 2\mu_{min}$, $\tau_1 = 0.238$ (1/day), $\tau_a = 1$, $\lambda_1 = \frac{1}{17}$ (1/day), $\lambda_2 = \frac{1}{20}$ (1/day), $p = .9$, $m = 0.2$, $\mu_h = 10^{-5}$, $\rho = 2$, and $H = 12000$. $\sum_{i=1}^{9}\mu'_h x_i(t)$ into $D(t)$ denotes that the population that move out of the other 9 compartments due to hospital saturation are added to the death compartment [34]. Control intervention $u(t)$ is assumed to alter $\beta(t)$, where $\beta(t) = (1-u(t))\big(\beta_0(I_{am}(t) + I_{as}(t)) + \beta_0(I_m(t) + mI_s(t))\big)$, $\beta_0 = 2.24 \times 10^{-9}$.

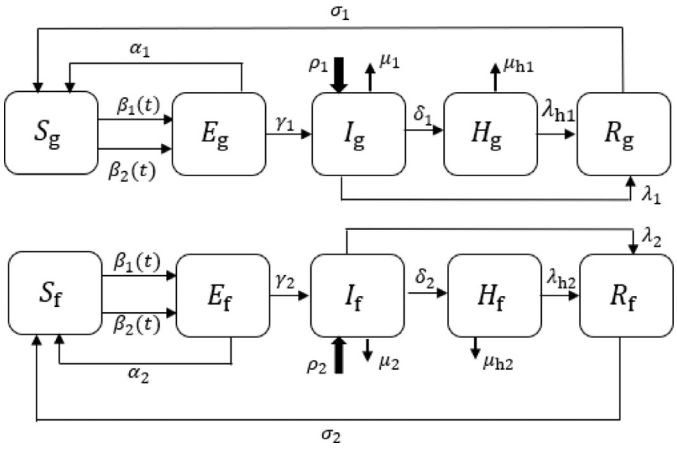

Fig. 7. Model 4: Mathematical model of COVID-19 that models differential disease transmission in frontliners and general public, $\beta_1(t) = \beta_{10}\frac{I_g(t)}{N(t)}$, $\beta_2(t) = \beta_{20}\frac{I_f(t)}{N(t)}$, $\beta_{i0} = \frac{R_{0i}(S_g(0)+E_g(0)+I_g(0)+S_f(0)+E_f(0)+I_f(0))}{\tau(S_g(0)+S_f(0))}$, $i = 1, 2$, $R_{01} = 2.5$, $R_{02} = 10$, $\tau_{in} = 14$ days, $S_g(0) = 100,000$, $S_f(0) = 1000$, $E_f(0) = 100$, $I_g(0) = 10$, $E_g(0) = I_f(0) = 0$, $H_i(0) = R_i(0) = 0$, $\alpha_i = 0 - 0.9$, $\gamma_i = 10/14$, $\delta_i = 0.01/14$, $\rho_i = 0.1$, $\mu_i = 0.03/14$, $\sigma_i = 0.1/30$, $\lambda_{hi} = 0.98/14$, $\lambda_i = 0.96/14$, and $\mu_{hi} = 0.02/14$, $i = 1, 2$ [22].

tine [99]. In [99], this model is used for forecasting the disease transmission in 5 regions in China and control intervention is not modeled.

4.3. Scenario: differential disease severity and ICU saturation

An important concern related to COVID-19 is the overwhelming of hospitals due to severely infected patients which results in direct and indirect deaths related to COVID-19 [94]. Policymakers estimated the threshold of infection above which the hospitals become saturated with the help of mathematical models such as that shown in Fig. 6. The increase in mortality due to hospital saturation is accounted for by including hospital capacity H and the death due to hospital saturation μ'_h in the model, where $\mu'_h = \mu_h$, if $I_s(t) \geq H$, $\mu'_h = 0$, if $I_s(t) < H$, and $\mu = \mu_{min}$, if $I_s(t) < H$, $\mu = \mu_{max}$ if $I_s(t) \geq H$ (Fig. 6), which implies that, the death increases whenever the number of severely infected cases goes beyond the hospital capacity H. Such a model can be used to derive active control intervention that keeps the value of $I_s(t)$ below H. This model also accounts for the import of infected cases to a country at a rate of ρ per day [34].

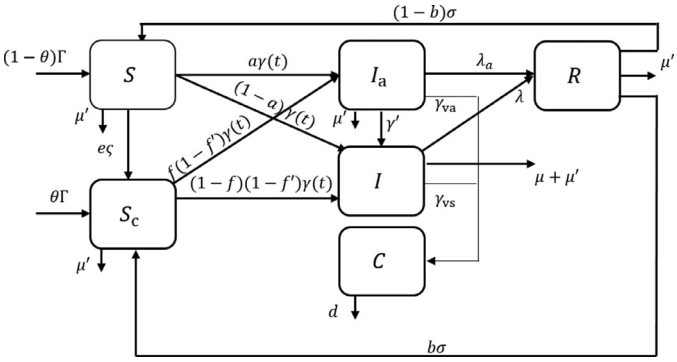

Fig. 8. Model 5: Mathematical model of COVID-19 with reinfection, compliant subpopulation, and viral concentration on contaminated surfaces [59]. $N(0) = 59.2 \times 10^6$, $N(t) = S(t) + S_c(t) + I_a + I(t) + R(t)$, $\lambda = 0.0499$ (1/day), $\lambda_a = 0.0749$ (1/day), $\theta = 0.5999$, $\Gamma = \mu' N(0) = 2113.44$ (persons/day), $\varsigma = 0.6499$ (intensity/day), $e(\gamma) = \frac{\gamma^n}{\gamma_0^n + \gamma^n}$, $b = 0.6337$, $\sigma = 2.74 \times 10^{-6}$ (1/day), $a = 0.6503$, $f = 0.8669$, $f' = 0.1499$, $\gamma' = 0.2499$ (1/day), $\gamma_{va} = 0.1019$ (pathogens/person/day), $\gamma_{vs} = 0.4315$ (pathogens/person/day), $d = 0.7525$ (1/day), $\mu = 0.11$ (1/day), $\mu' = 3.57 \times 10^{-5}$ (1/day), and $C_{50} = 2091775$ (pathogens). Control intervention $u_1(t)$ (effect of social distancing) and $u_2(t)$ (effect of disinfecting the environment) are assumed to alter $\gamma(t)$, where $\gamma(t) = (1-u_1(t))\beta\big(\frac{I(t)+u_2(t)I_a(t)}{N(t)}\big) + (1-u_2(t))\beta_{ch}\big(\frac{C(t)}{C(t)+C_{50}}\big)$, $\beta = 0.27$ (contacts/day), $\beta_{ch} = 0.00101$ (contacts/day), $u_1(t) = 0 - 1\%$ and $u_2(t) = 2.663$ (1.1 – 3) [59].

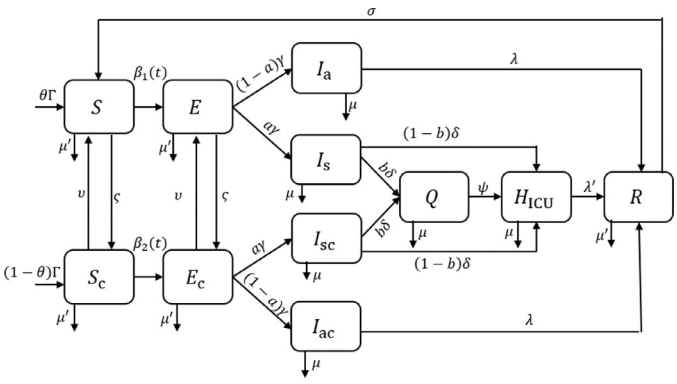

Fig. 9. Model 6: Mathematical model of COVID-19 that accounts for social behavior of compliant subpopulation. $N(0) = 3,000,282$, $S(0) = 3 \times 10^6$, $S_c(0) = 200$, $E(0) = 40$, $E_c(0) = 40$, $I_a(0) = 2$, and the initial condition for all other compartments is 0, $R_0 =< 1$, $\delta = 1/7$ (1/day), $\lambda = 0.0714$ (1/day)), $\lambda' = 0.0714$ (1/day), $\psi = 0.002$ (1/day), $\mu = 0.02$ (1/day), $\mu' = 1/(365 \times 50)$ (1/day), $\sigma = 0.2$ (1/day), $\Gamma = 100$ (1/day), $\zeta = 1$ (1/day), $\upsilon = 0.1$ (1/day), $\theta = 1/7$ (1/day), $\gamma_s = 0.86834$ (1/day), $a = 0.8683$, and $b = 0.4$. Control interventions $u_1(t)$ (effect of quarantine) and $u_2(t)$ (effect of isolation) are assumed to alter $\beta_1(t) = \frac{\beta_0(u_1(t)m_q Q(t) + m_a I_a(t) + m_s I_s(t) + u_2(t)m_h H_{ICU}(t))}{N(t) - (1-u_1(t))Q(t) - (1-u_2(t))H_{ICU}(t)}$, $\beta_2(t) = \frac{\beta_0(m_{ac}I_{ac}(t) + m_{sc}I_{sc}(t) + u_2(t)m_h H_{ICU}(t))}{N(t) - Q(t) - (1-u_2(t))H_{ICU}(t)}$, where $m_q = 0.3 \times 7/3$, $m_a = 0.425 \times 7/3$, $m_s = 0.425 \times 7/3$, $m_{ac} = 0.225 \times 7/4$, $m_{sc} = 0.3 \times 7/3$, and $m_h = 0.57 \times 7/4$ [64].

4.4. Scenario: differential disease transmission among frontliners and general public

The interaction rate of hospital staff, workers in supermarkets, and police is considerably higher compared to the general public. To analyze the influence of such differential disease transmission in the overall dynamics, in Buhat et al. [22], the dynamics of frontliners and the general public are modeled separately.

As shown in Fig. 7, the mean protection level (α_i, $i = 1, 2$), possibility of reinfection (σ_i, $i = 1, 2$), import of cases (ρ_i, $i = 1, 2$) and hospitalization rate (δ_i, $i = 1, 2$) of public and frontliners are accounted for in this model. Using model-based analysis, it is concluded that protecting frontliners is important to make sure that they are available for the treatment of the general public, however, protecting them alone does not flatten the curve [22]. Similar to the model shown in Fig. 6, the model in Fig. 7 can be used

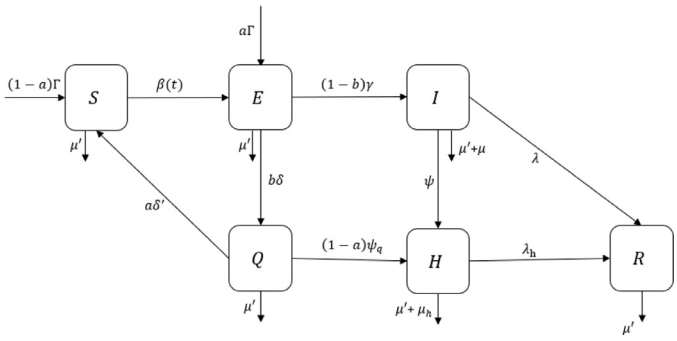

Fig. 10. Model 7: Mathematical model of COVID-19 that accounts for the influence of public health education, quarantine and hospitalization. $S(0) = 12 \times 10^6$, $E(0) = 1565$, $Q(0) = 800$, $I(0) = 695$, $H(0) = 326$, and $R(0) = 200$, $\lambda = 0.03521$ (1/day), $\lambda_h = 0.04255$ (1/day), $\mu = 0.0079$ (1/day), $\mu_h = 0.0068$ (1/day), $\mu' = 0.000034$ (1/day), $\Gamma = 600$ (1/day), $\delta' = 0.07143$ (1/day), $\psi = 0.1327$ (1/day), $\psi_q = 0.1259$ (1/day), $R_0 = 1.51$ when the exposed population is not quarantined, while $R_0 = 0.76$ when all of them are on quarantine, and $R_0 = 2.5$ when the infected individuals are not quarantined or isolated. Control intervention $u(t)$ is assumed to alter $\beta(t)$, where $\beta(t) = (1 - u(t))\frac{\beta_0(I(t)+m_e E(t)+m_q Q(t)+m_h H(t))}{N(t)}$, $\beta_0 = 0.25$ (1/day), $u(t) = [0, 1]$, $m_e = 0.3$, and $m_h = m_q = 0.1$, [76].

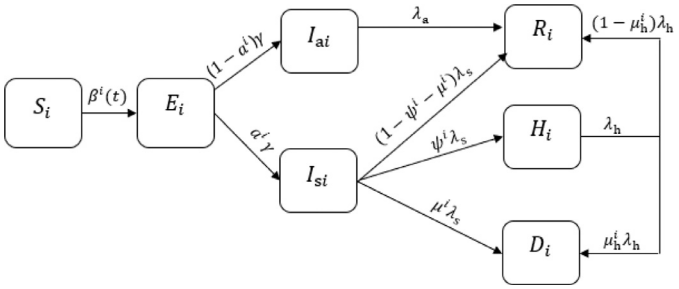

Fig. 11. Model 8: Mathematical model of COVID-19 that accounts for age-wise interaction rates. The parameters are estimated for 9 age groups such as 0–9, 10–19, 20–29, 30–39, 40–49, 50–59, 60–69, 70–79, and ≥ 80, for $i = 1, 2 \ldots, 9$, respectively, $\beta^i(t) = \phi \sum_{j=1}^{9} A(i, j) \frac{I_j^j(t)}{N^j} + \phi \sum_{j=1}^{9} A(i, j) \frac{I_s^j(t)}{N^j}$, $\tau_{in} = \frac{1}{\gamma} = 5$, $\tau_a = \frac{1}{\lambda_a} = 4$, $\tau_s = \frac{1}{\lambda_s} = 10$, $\tau_h = \frac{1}{\lambda_h} = 10.4$ (days). $N^1 = 12\%$, $N^i = 13\%$, $i = 2, \ldots, 5$, $N^6 = 14\%$, $N^7 = 12\%$, $N^8 = 7\%$, $N^9 = 4\%$, $a^1 = 11.1\%$, $a^i = 12.1\%$, $i = 2, \ldots, 5$, $a^6 = 17.5\%$, $a^i = 28.7\%$, $i = 7, 8, 9$, $\psi^1 = 18.2\%$, $\psi^2 = 5.5\%$, $\psi^3 = 6.8\%$, $\psi^i = 13.9\%$, $i = 4, 5$, $\psi^6 = 25.1\%$, $\psi^i = 51.2\%$, $i = 7, 8$, $\psi^9 = 61.7\%$, $\mu_h^i = 0.2\%$, $i = 1, 3$, $\mu_h^2 = 0\%$, $\mu_h^i = 0.9\%$, $i = 4, 5$, $\mu_h^6 = 3.6\%$, $\mu_h^i = 14.9\%$, $i = 7, 8$, $\mu_h^9 = 32.8\%$, $\mu^i = 0.1\%$, $i = 1, 3$, $\mu^2 = 0\%$, $\mu^i = 0.4\%$, $i = 4, 5$, $\mu^6 = 1.4\%$, $\mu^i = 5.9\%$, $i = 7, 8$, and $\mu^9 = 12.9\%$ [41].

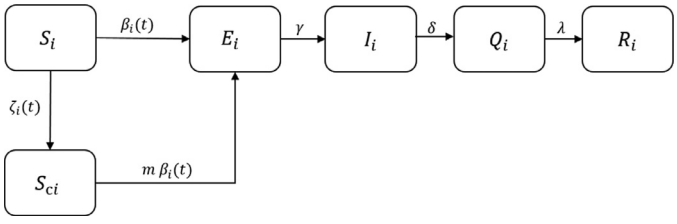

Fig. 12. Model 9: Mathematical model of COVID-19 that model how school opening delay will affect the pandemic, $\beta_i(t) = \sum_{j=1,2} \beta_{0ij} \frac{I_{j(t)}}{N_j(t)}$, where $\beta_{0ij} = \begin{pmatrix} 7.991 & 0.7172 \\ 0.7172 & 4.7531 \end{pmatrix}$, $\beta_{0ij} = \begin{pmatrix} 7.8192 & 0.8544 \\ 0.8544 & 4.6452 \end{pmatrix}$, $\beta_{ij}^0 = \begin{pmatrix} 8.5531 & 1.0558 \\ 1.0558 & 5.0616 \end{pmatrix}$ represent transmission matrices for Data 1, Data 2, and Data 3, respectively, $\zeta_i(t) = \zeta_{0i}(1 - e^{-eQ_i(t)})$, $e = 0.001$, $\zeta_{01} = 1.8138$ (1/day), $\zeta_{02} = 1.69$ (1/day), and $\zeta_{03} = 2.121$ (1/day), for Data 1, Data 2, and Data 3, respectively, $m = 0.02$, $\lambda = 1/14$ (1/day), $\delta = 1/4$ (1/day), and $\gamma = 1/4.1$ (1/day) [62].

to evaluate the threshold of hospital saturation and the impact of import of infected cases. In [22], parameter sensitivity analysis is conducted to study the influence of various model parameters on disease transmission while control intervention is not modeled explicitly. However, this model does not quantify how far the infection of frontliners, especially medical staff, affects the services provided in a hospital.

4.5. Scenario: impact of viral shedding and reinfection

The scenarios that can be analyzed using Model 5 depicted in Fig. 8 include the impact of viral shedding to the surrounding, compliance rate of public, and reinfection on the disease transmission. In [59], the influence of educated people $S_c(t)$, who comply with the regulations, and the disease transmission dynamics with respect to the concentration of viral particles $C(t)$ on contaminated surfaces or environment is incorporated. Transmission from human to human (β) and contaminated surface to human (β_{ch}) are accounted for in the model shown in Fig. 8. To assess the influence of social distancing and disinfection of surrounding contaminated surface, the model given in Fig. 8 is modified to a mixed-delay model with incubation delay and additional quarantine compartments [59]. See supplementary file for model equations for Fig. 8 and modified model equations with incubation delay and additional quarantine compartments. Using the model-based analysis, it is shown that, if there is a possibility of reinfection (i.e. no permanent immunity for recovered), then there exists a backward bifurcation (co-existence of endemic and disease-free equilibria) at $R_0 = 1$ [131]. However, if the recovered patients achieve permanent immunity, then there is no backward bifurcation and disease-free equilibria is globally asymptotically stable for $R_0 < 1$. It is also noted that if there is permanent immunity, (i.e. with reinfection rate, $\sigma = 0$) then reducing $R_0 < 1$ is enough to contain the disease, however for $\sigma \neq 0$ (no permanent immunity) reducing R_0 below the threshold ($R_0 < 1$) is not enough to contain the disease. The model-based intervention analysis also points to the importance of reducing the transmission of disease via asymptomatic but infectious subpopulation at least by 30% and via symptomatic patients at least by 50% for controlling disease spread.

4.6. Scenario: social behavior of compliant subpopulation

The positivity and well-posedness of the mathematical model of COVID-19 that is given in Fig. 9 are investigated in Kouakep et al. [64]. It can be seen from Fig. 9, that the contribution of quarantine (home) and isolation (hospitalised in ICUs) measures on the overall disease transmission is modeled using $u_1(t)$ and $u_2(t)$, where $u_1(t) = 0$ denotes perfect quarantine (infeasible), $u_1(t) = 1$ denotes least effective quarantine, $u_2(t) = 0$ denotes perfect isolation, and $u_1(t) = 0.8$ denotes least effective isolation. The model-based analysis accurately predicted that the infection peaks by June 2020 in Cameroon if necessary preventive and containment measures are not taken. This model also studies the impact of possible reinfection in the community. Similarly, in Victor [128], using a modified SEIQRS model that accounts for reinfection, it is shown that the disease-free equilibrium does not satisfy conditions for local or global asymptotic stability. This implies that with possible cases of reinfection and in the absence of a protective vaccine, it is hard to get rid of the virus from this world. At the time of the study reported in Kouakep et al. [64], the significance of re-infection was yet to be known. Later on many scientific studies remarked that reinfection is insignificant (0.01% (0.01–0.02%)) [5,6]. This is not to say that re-infection does not exist [37,44,95]. Even though less in proportion, there are some notable reports of reinfection that points out more severe disease in case of re-infection compared to the first infection [52].

4.7. Scenario: influence of public health education, quarantine, and hospitalization

In [76], a mathematical model of COVID-19 that accounts for the influence of public health education, quarantine, and hospitalization is discussed. The model is well-posed and based on the Pontryagins minimum principle, it is concluded that the NPI gives

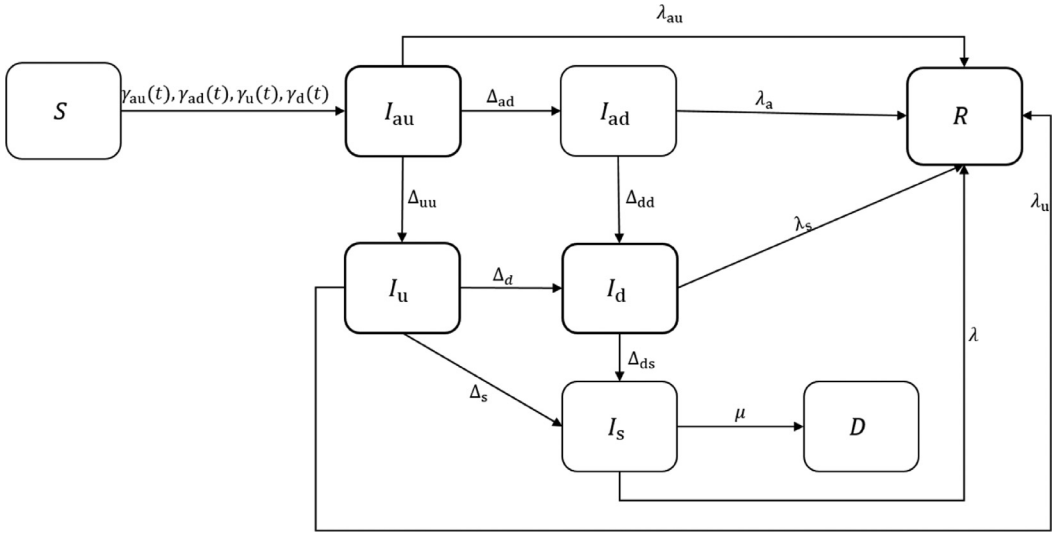

Fig. 13. Model 10: Mathematical model of COVID-19 that accounts for undetected, detected, symptomatic, asymptomatic, and severely ill cases, where, $\gamma_{au} = \gamma_{au0} I_{au}(t)$, $\gamma_{ad} = \gamma_{ad0} I_{ad}(t)$, $\gamma_u = \gamma_{u0} I_u(t)$, $\gamma_d = \gamma_{d0} I_s(t)$, $S(0) = 1 - I_{au}(0) - I_{ad}(0) - I_u(0) - I_d(0) - I_s(0) - R(0) - D(0)$, $I_{au}(0) = 200/(60 \times 10^6)$, $I_{ad}(0) = 20/(60 \times 10^6)$, $I_u(0) = 1/(60 \times 10^6)$, $I_d(0) = 2/(60 \times 10^6)$, $I_s(0) = R(0) = D(0) = 0$. Parameter values are estimated for 6 different stages of interventions. On Day 1, $\gamma_{au0} = 0.57$, $\gamma_{ad0} = \gamma_{d0} = 0.011$, $\gamma_{u0} = 0.456$, $\Delta_{ad} = 0.171$, $\Delta_{uu} = \Delta_{dd} = 0.125$, $\lambda_{au} = \lambda_a = 0.034$, $\Delta_d = 0.371$, $\Delta_s = \Delta_u = \lambda_s = \lambda_u = 0.017$, $\Delta_{ds} = 0.027$, $\mu = 0.01$, and $R_0 = 2.38$. After Day 4, with hand washing and social distancing measures, $\gamma_{au0} = 0.422$, $\gamma_{ad0} = \gamma_{d0} = 0.0057$, $\gamma_{u0} = 0.285$, and $R_e = 1.66$. After Day 12, with screening limited to individuals with symptoms, $\Delta_{ad} = 0.143$ and $R_e = 1.8$. After Day 22, with incomplete lockdown, $\gamma_{au0} = 0.36$, $\gamma_{ad0} = \gamma_{d0} = 0.005$, $\gamma_{u0} = 0.2$, $\Delta_{uu} = \Delta_{dd} = 0.034$, $\lambda_{au} = 0.08$, $\Delta_s = 0.008$, $\Delta_{ds} = 0.015$, $\lambda_a = 0.017$, and $R_e = 1.6$. After Day 28, with complete lockdown $\lambda_{au0} = 0.21$, $\gamma_{u0} = 0.11$, and $R_e = 0.99$. After Day 38, with mass testing campaigns, $\Delta_{ad} = 0.2$, $\Delta_{uu} = \Delta_{dd} = 0.025$, $\lambda_a = \lambda_s = \Delta_u = 0.02$, $\lambda = 0.01$, and $R_e = 0.85$ [43].

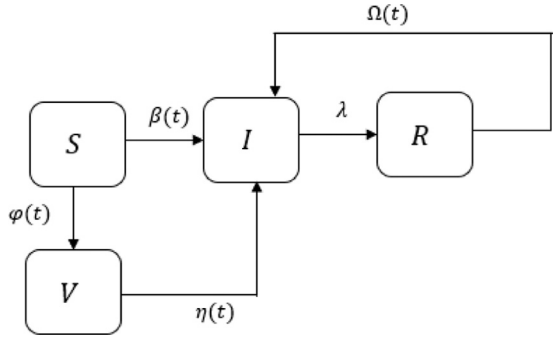

Fig. 14. Model 11: Mathematical model of COVID-19 that accounts for protection of a subpopulation by vaccination, $\beta(t) = \beta_0 I(t)$, $\Omega(t) = \Omega_0 \beta_0 I(t)$, $\varphi(t) = \varphi_0 + \varphi_{\Lambda_M}(t)$, $\varphi_{\Lambda_M}(t) = (1 - \varphi_0 - \varphi_1) \frac{M\Lambda_M(t)}{1 + M\Lambda_M(t)}$, $\dot{\Lambda}_M(t) = \Lambda_t(\Lambda_c I(t) - \Lambda_M(t))$, $\eta(t) = \eta_0 \beta_0 I(t)$, $\beta_0 = 1.07$ (1/person/days) $\lambda = 0.278$ (1/days), $\Lambda_t = (0.00833, \infty)$, $M = 500$, $1 - \varphi_1 = 0.99$, $\eta_0 = 0.15$, and $\Omega_0 = 0.2$ [24]. Control intervention $u(t) = \varphi(t)$, where $\varphi(t)$ is the vaccination rate.

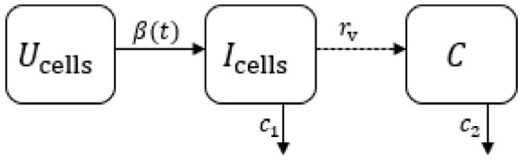

Fig. 15. Model 12: Mathematical model of COVID-19 that accounts for virus dynamics in a host. $U_{cells}(0) = 4 \times 10^8$ (cells), $I_{cells}(0) = 0$ (cells), and $C(0) = 0.31$ (copies/ml), $\beta(t) = \beta_v C(t)$, $\beta_v = 4.71 \times 10^8$ (ml/(copies.days)), $r_v = 3.07$ (((copies/ml)/days)/cells)), $c_1 = 1.07$ (1/days), and $c_2 = 2.4$ (1/days) [49].

the best results when implemented within 100 days of the disease outbreak and multiple interventions are imperative to reduce disease spread. Zero infection was not attained even with the combined implementation of three interventions. The control intervention $u(t)$ marked in Fig. 10 models the public health education. Note that the infection, recovery, or death of non-quarantined/nonhospitalized cases are also accounted for in this model. Model-based analysis reveals that the disease transmission reduces by half ($R_0 = 1.51$ to 0.76) when all the exposed individuals are quarantined and an infected individual can infect three other individuals ($R_0 = 2.5$) if not isolated or quarantined. Moreover, the simulation results show that even though three interventions together (public health education, quarantine, and hospitalization (isolation)) perform better than one or two interventions, it is not enough to bring down the cases to zero [76].

4.8. Scenario: age-wise interaction

Several studies investigated the significance of population heterogeneity and discrimination in age-wise interaction in COVID-19 transmission [13,20,41,78,102]. In [20], using an SEIR model, it is shown that as the proportion of infected individuals in groups with the highest contact rates is greater than that in groups with low contact rates, population heterogeneity can have a significant impact on the population-wide infection or vaccination rate required to curtail the spread [13,20,78].

In [41], a seven compartmental model of COVID-19 for various age groups is discussed. As shown in Fig. 11, 7 set of equations can be written for each of the 9 age groups (S_i, E_i, I_{ai}, I_{si}, R_i, H_i, D_i, $i = 1, \ldots, 9$) based on the parameters given in Fig. 11, where $A(i, j)$ denotes the number of contacts between age group j and i and $N^i(t)$ is the population size in each age group in New Jersey. The main feature of this model is the use of social interaction data at home, work, and school to quantify the mean contact rates of each age group. Control intervention is not explicitly modeled in Forgoston and Thorne [41], instead empirically derived contact information is used to study the effect of lockdown and school reopening in New Jersey. Based on the study, it is pointed out that the oldest age group constitutes the smallest proportion of the total population and hence contributes to the smallest number of infected cases. However, the maximum death (32.8% of hospitalized) is associated with the oldest age group.

Using the model depicted in Fig. 11, it is pointed out that, rigorous testing, contact tracing, and isolation of infected are imper-

ative to reduce disease transmission and thereby ease lockdowns. Similar to the results in Fang et al. [38], Lahiri et al. [68], it is highlighted in Forgoston and Thorne [41] that early lockdown can reduce overall death only if rigorous testing, contact tracing, and isolation are carried out while easing lockdowns, otherwise the overall death will increase due to second waves. A study that used a model that accounts for age-wise interaction and heterogeneities in population models suggest that herd immunity can be achieved with a population-wide infection rate of 40%. This is considerably lower (earlier 60%) than previous estimates [20]. The model discussed in Fig. 11 can be extended by adding a vaccinated population compartment to investigate the effect of age-wise homogeneity/heterogeneity in vaccine efficacy in the overall control of the disease.

4.9. Scenario: impact of closing/re-opening of schools and colleges

Compliance of the population with policies and restrictions imposed by the epidemic control authorities is very important for the containment of an epidemic. However, children in the age of 5–15 are less likely to comply with the rules and thus risking self-protection when at school. Even though susceptibility of individuals less than 20 years old is half of the adults [25,87,102], the fact that if infected, clinical symptoms are manifested only in 21% of children increase the overall disease transmission as hidden/unidentified infected children can act as carriers [33]. Moreover, many recent studies point out the emerging clinical spectrum of COVID-19 in children, suggesting significant (19.40–36.80%) hospitalization of infected children and a small proportion has developed severe complications including encephalopathies, inflammatory CNS (central nervous system), ischemic stroke, and other neurological complications [19,30,54,60,98,104]. In case of earlier pandemics (influenza, 2009) also it was reported that school closure has reduced transmission among children by 86% (44%99%) [14,53,62]. Thus, school closure is one common mitigation strategy implemented against COVID-19 in most countries. However, loss of school days is a concern and some studies suggest that school closure for 4–12 weeks can affect GDP in UK and US by 0.15 to 0.3% [45,69,110].

In [62], a modified SEIR model is used to investigate the impact of school closure over a period of time as a NPI mitigation strategy against COVID-19 spread. This study considered two age groups namely children $(0-19)$ and adults (≥ 20). The compartments S_{ci}, $i=1,2$ shown in Fig. 12 model the sub-population with behavioral changes due to awareness/education about the disease, where $i=1,2$ correspond to children and adults, respectively. In Fig. 12, $\zeta_i(t)=\zeta_{0i}(1-\mathrm{e}^{-eQ_i(t)})$, e is a scaling parameter that models the increased movement of people from $S_i(t)\rightarrow S_{ci}(t)$ due to the increased awareness/behavioral change. Also note that as the number of people isolated, quarantined, or working from home increases, the movement into the complaint compartment $(S_{ci}(t))$ increases. Using a transmission matrix β_{ij}, $i=j=1,2$, the disease transmission among children $(i=1,j=1)$, among adults $(i=2,j=2)$, and inter-group transmission $(i=1,j=2$ and $i=2,j=1)$ are modeled. Control intervention is not explicitly modeled in Kim et al. [62], instead empirically derived information is used to study the effect of school reopening in Korea. The impact of delayed school re-opening is studied by estimating the transmission matrix using three sets of data, namely Data 1 (February 16 to March 2), Data 2 (February 16, to March 9), and Data 3 (February 16 to March 22). For all the three data set, it can be seen from the value of β_{ij} given in Fig. 12 that the intra-group transmission is more than inter-group transmission $(\beta_{ij,i=j}>\beta_{ij,i\neq j})$. Simulation studies are conducted with the assumption that the school re-opening can result in 10 and 30 times increase in the disease transmission and it is concluded that school closure or delayed (1-month delay) reopening can reduce up to 60 and 255 cases, respectively.

Similar results are reported in Karatayev et al. [58], Kim et al. [62], Phillips et al. [100]. In [100], the outbreak size and student-days lost due to school closure in Ontario childcare centers and primary schools are studied. Based on the study, it is proposed that for childcare and primary school, reopening safety can be enhanced by switching to lower student ratios. In another study, reported in Kim et al. [62], data from Korean-CDC is used to model children and adult groups. Assuming the transmission rate between children groups would be increasing many folds after the schools open, in Korea, approximately additional 60 cases are expected to occur from March 2, to March 9, and approximately additional 100 children cases are expected from March 9, to March 23. After 3 weeks, i.e. by March 23, the number of expected cases for children is 28.4 for 7 days and 33.6 for 14 days. After 3 weeks, the possibility for massive transmission between groups is less and within-group transmission is more due to increased compliance to rules [62]. In [102], projections suggest that premature and sudden lifting of interventions could lead to an earlier secondary peak, which could be flattened by relaxing the interventions gradually. In general, the guidelines for school re-opening include disinfecting (α increases, β and γ decreases), screening (β and γ decreases), ventilation (γ decreases), no sharing and interaction (β and γ decreases), wearing mask/gloves (α increases, β and γ decreases). See Fig. 3 for model parameters that are affected by various interventions.

4.10. Scenario: influence of mass testing

In [43], the proportion of population which remain undetected, detected, symptomatic, asymptomatic, and severely ill are modeled based on the population data of Italy. Fig. 13 shows the schematic diagram of the modified SIR model discussed in Giordano et al. [43]. As a proportion (34%) of total cases go undetected, the total number of cases are often underestimated [43]. Note that in this model, $\gamma_{\mathrm{au0}}>\gamma_{\mathrm{u0}}$, account for the fact that, even though undetected, susceptible population are more likely to avoid direct contacts with those who are showing some symptoms relevant to an ongoing pandemic. Similarly, $\gamma_{\mathrm{au0}},\gamma_{\mathrm{u0}}>\gamma_{\mathrm{ad0}},\gamma_{\mathrm{d0}}$ as detected cases are more likely to be under quarantine/isolation. In [43], as shown in Fig. 13, parameters are estimated for 6 different stages of interventions. It can be seen that after Day 4, the values of infection rates γ_{ad0}, γ_{d0}, γ_{au0}, and γ_{u0} have reduced due to the social distancing measures and epidemic awareness. Similarly, after Day 38 the detection rate of asymptomatic patients have increased due to mass testing campaigns (Δ_{ad}). To better understand the epidemic behavior under various control interventions, the 8 compartmental system shown in Fig. 13 is divided into three subsystems such $x_1(t)=S(t)$, $x_2(t)=[I_{\mathrm{au}}(t),I_{\mathrm{ad}}(t),I_{\mathrm{u}}(t),I_{\mathrm{d}}(t),I_{\mathrm{s}}(t)]'$, and $x_3(t)=[R(t),D(t)]'$, where $[\ ]'$ denote matrix transpose. Model-based analysis, reveals that $R(t)$ and $D(t)$ monotonically increases as epidemic progresses and only when $I_{\mathrm{au}}(t)+I_{\mathrm{ad}}(t)+I_{\mathrm{u}}(t)+I_{\mathrm{d}}(t)+I_{\mathrm{s}}(t)=0$, (that is when total known and unknown infected are zero), $S(t)$, $R(t)$, and $D(t)$ are at equilibrium. Specifically, as the control measures directly depend on the number of infected cases, $\dot{x}_2(t)=Fx_2(t)+Bu(t)$ is defined where $F\in\mathbb{R}^{5\times5}$, $B\in\mathbb{R}^{5\times1}$, and $u(t)\in\mathbb{R}$, $u(t)=(\gamma_{\mathrm{au}}I_{\mathrm{au}}(t)+\gamma_{\mathrm{ad}}I_{\mathrm{ad}}(t)+\gamma_{\mathrm{u}}I_{\mathrm{u}}(t)+\gamma_{\mathrm{d}}I_{\mathrm{d}}(t))S(t)$. Model-based analysis points out that necessary social-distancing measures should be implemented early, and lockdown measures can be relaxed only after making sure that mass testing and quarantining efforts are in place. This paper also points out the misconception of case fatality rate due to undetected cases (actual CFR=9.8%, earlier estimate of CFR=13%) which highlight the importance of diagnostic campaigns.

4.11. Scenario: vaccination

During the beginning of the pandemic even when it was not certain whether a vaccine can be developed or not, many mathematical model-based analysis published motivating results highlighting that even a moderately effective vaccine can have a significant impact in reducing the transmission rate [34,78,91,91,92]. Presently, the world is breathing a sigh of relief as the question on the possibility of vaccine and efficacy of the vaccine is already answered with the development of as many as 3 vaccines (with $>$ 80% efficacy) [26,77]. However, we need to wait to know the assured period of protection with the use of vaccines and the presence of any side effects in the long run [35].

In [24], an SIR model with vaccination compartment is used for studying vaccination impact. In Fig. 14, Λ_c represents the media coverage that leads to dissemination of information and the number of infections reported by the public health system. All this information influences the vaccination decision of the population. A Michaelis–Menten form of equation is used to represent the saturation in $\varphi_{\Lambda_M}(t)$, where $\varphi_{\Lambda_M}(t)$ denotes the information-based vaccination rate, $M = 500$ is used to model a 96.4% vaccination coverage when the information index $\Lambda_M(t) = 0.07$. Similarly, in Mukandavire et al. [91], an SEIR model is used to study vaccination where the vaccination coverage, V_c follows the relation $V_c \geq (1 - 1/R_0)/s$, where $R_0 = 2.95$ (2.83–3.33) and s is the reduction in susceptibility due to immunization [91].

As confirmed cases of reinfection are reported, everyone is curious to know how long the duration of the acquired immunity due to infection or vaccination stays. In [5], out of 133,266 laboratory-confirmed COVID-19 cases, 0.18% were tested again 45 days after the first positive swab. Out of the 0.18%, (i.e. 54 cases), 1 person was hospitalized with a relatively mild infection. Based on this data, the risk of reinfection is 0.01% (0.01–0.02%) and the incidence rate of reinfection is 0.36 (0.28–0.47) per 10,000 person-weeks suggesting a strong protective immunity at least for a few months after primary infection [5]. In general, the concerns and challenges related to vaccination include (i) safety of vaccine and severity of side effects if any, (ii) efficacy of the vaccine, (iii) cost of vaccine and distribution, (iv) duration of protection, (v) vaccine hesitancy, and (vi) prioritizing vaccine distribution [13,81]. Along with the elderly and severely sick, individuals with high social interaction (frontliners) should also be on the priority vaccination list.

4.12. Virus dynamics

While most of the mathematical models that are in the literature related to COVID-19 focus on the disease transmission dynamics in a population, few literature report models that account for the clinical/biological aspects of the virus [49]. This is primarily due to the fact that virological models are more relevant when preventive (prophylactic) vaccines or curative drugs are available.

Fig. 15 shows the schematic of an ODE model used to represent the virus dynamics in a host, where $U_{\text{cells}}(t)$ is the uninfected susceptible (target for the virus) cells, $C(t)$ is the concentration of virus, β_v is the rate at which uninfected cells gets infected, r_v is the rate at which infected cells release infectious viral particles, and c_i, $i = 1, 2$ are the clearance rates of infected cells and viral particles, respectively [49]. This model can be extended further by adding immune response dynamics and drug-specific (control intervention) dynamics.

4.13. Cumulative model

Even though mechanistic epidemic models allow better analysis of the influence of parameters and the response to control interventions such as scenarios like the cost of isolation alone, vaccination alone, or mixed, etc., phenomenological models (cumulative models) are useful for the prediction of global trends [51,75]. Logistic and Richard's models are cumulative epidemic models that are predicated on the assumption of uniformity of population. Logistic model represents the initial exponential increase in disease transmission followed by saturation as given by

$$\dot{X}(t) = \kappa X(t)\left(1 - \frac{X(t)}{K}\right), \tag{2}$$

where $X(t)$ is the cumulative incidence, κ is the exponential increase in $K = \lim_{t\to\infty} X(t)$. Richards model is a modified logistic model (power law) such as

$$\dot{X}(t) = \kappa X(t)\left(1 - \frac{X(t)}{K}\right)^n, \tag{3}$$

where n is the steepness of the curve.

Another set of cumulative models that are used to study COVID-19 disease transmission characteristics are the functional data analysis (FDA) models which are statistical models [28,66,118]. Unlike other statistical models that rely on sample data points, FDA models are built on the shape of disease transmission curve (time dynamics) and are used to figure out latent information if any in the whole set of data. For instance, the FDA model discussed in Carroll et al. [28] is given by

$$\begin{aligned}\dot{X}(t) =& \Pi_0(t) + \Pi_1(t)X(t) + \Pi_2(t)\varkappa + \Pi_3(t)\varpi \\ &+ \Pi_4(t)W(t-\tau) + Z(t),\end{aligned} \tag{4}$$

where $X(t)$ is the cumulative number of cases, $W(t-\tau)$ denotes delayed reduction in workplace mobility, $Z(t)$ accounts for error (mean-zero stochastic drift), $\Pi_i(t)$, $i = 0, \ldots, 4$ are the time varying regression coefficients, $\varkappa$ is the population density, and ϖ is the proportion of elderly population (age $>$ 65). FDA models were used to (1) identify dominant incidence curves, (2) enable easy classification/clustering of a data set, and (3) analyze reasons behind differential COVID-mitigation outcome reported in different countries despite the deployment of similar NPIs [28,66,118]. With respect to the general model (1) and Fig. 1, the model (2)–(4) corresponds to a single compartment model ($X(t) = x_1(t)$) which represents the cumulative number of cases or the infected population ($I(t)$) whose dynamics is influenced by various time varying factors such as, disease transmission rate, population density, workplace mobility, etc. For instance, (2) can be written as $\dot{X}(t) = r(t)X(t)$, where $r(t) = \kappa\left(1 - \frac{X(t)}{K}\right)$. Note that compared to the deterministic compartmental models, FDA models additionally accommodate stochasticity involved in epidemic dynamics.

5. Active control of pharmaceutical and nonpharmaceutical interventions

The use of optimal, model predictive, sliding mode, adaptive, and fuzzy logic-based controllers have been studied for epidemic control and vaccination deployment of earlier pandemics [7–10,113,115,127]. Testing various control interventions are straight forward application of mathematical models [119]. Given that there exists a vast set of possible interventions and combinations of interventions, it is desirable to figure out the reliable combination of interventions and control strategies. It is quite obvious that single-interventions such as implementing $>$99% border closing, or tracing $>$70% contact tracing or significantly limiting the contact time of health care professionals ($<$9 hours) with an infected person, etc., are infeasible in a current socio-economic setting [48,103,116].

Cost-effectiveness of various intervention strategies is also a subject of study [56,112]. It should be noted that "effectiveness"

Table 6
Control theoretic approaches used for COVID-19.

Model [ref]	Control method	Remark
Modified SEIR model [34]	Optimal control	Model accounted for differential disease severity. Optimal control solution derived under the objective of minimizing hospital saturation and COVID-19 related death. The optimal solution suggests to progressively increase the control until the fourth month (maximum control) of the epidemics and then steadily decrease the control until vaccine deployment.
Modified SIR model [50]	Optimal control	Accounted for limited resource availability and economic cost associated with restricted inter-regional mobility. The optimal control policy that combines early detection/testing and lockdown methods in each region is obtained. Intensive mitigation strategies, with higher daily resource usage and shorter duration, are suggested for effective control of disease in the under-resourced regions.
Modified SEIR model [135]	Optimal control	Imposing constant control in the range of 90% to 100%. NPIs for control include staying home, hygiene habits, sanitization, and quick detection.
Modified SIR and SEIR model [12]	Optimal control	Closed-loop control considering delay in loop. A closed-form solution for active optimal intervention is derived.
Modified SIR model [27]	Model predictive control	Optimal use of NPIs in post lockdown period for a multi-region scenario with hospital saturation constraint
Modified SEIR[93]	Sliding mode control	Closed-loop constrained control. A day by day reduction in the contact rate is suggested to constraint the severely infected so as not to cross ICU capacity.

and "cost-effectiveness" of intervention have disparate implications, lockdown is a very effective intervention but not at all cost-effective. Based on 62 evidence-based research studied in Juneau et al. [56], it is concluded that

- Contact tracing, protecting frontliners and vulnerable population, and isolation of infected are the most cost-effective interventions,
- Home quarantine, school/workplace closures are effective but costly, and
- Interventions are more effective when adopted early and implemented in combinations.

Table 6 summarizes the control-theoretic approaches that are used to mitigate COVID-19. In [34], a modified SEIR model-based optimal control strategy to deploy strict public-health measures until the availability of a vaccine is discussed. The derived optimal solution is more effective compared to constant-strict control measures and cyclic control measures. In Fig. 6, in Djidjou-Demasse et al. [34], $\beta(t) = (1-u(t))\big(\beta_0(I_{\text{am}}(t)+I_{\text{as}}(t))+\beta_0(I_{\text{m}}(t)+mI_{\text{s}}(t))\big)$, where $u(t)$ accounts for NPIs in range [0,1]. The derived optimal solution is more effective compared to constant-strict control measures and cyclic control measures.

In [50], an extended SIR model that considers mobility from highly infected to mildly infected region, limited resource availability, and economic burden associated with limiting cross-region mobility is studied. As mentioned in Fig. 4, the relation $\gamma_i(t) = \gamma_0(1-u_i(t))^2 S_i(t) I_i(t)$, $i = A, B$, is used to account for the influence of early detection/testing and lockdown methods in region A and B, where $u_i(t)$ represents combination of lockdown and quarantine. This study reveals that optimal policy depends on the time duration of the restriction, resource availability, and human mobility across regions. Intensive mitigation strategies, with higher daily resource usage and shorter duration, are suggested for effective control of disease in the under-resourced regions [50].

In [135], a modified SEIR model is used to derive optimal control solution with respect to four NPIs. Specifically, the control inputs $u_i(t)$, $i = 1, \ldots, 4$, represent stay home, hygiene habits (face mask and hand wash), quick case detection by PCR test, and use of sanitizers to disinfect contaminated surfaces, respectively. The modified SEIR model included compartments for asymptomatic infected, quarantined, and hospitalized. Two additional compartments that model the food items or other kinds of stuff that humans use/consume in a day to day life and contaminated food items or other stuffs due to interaction with asymptomatic infected, symptomatic infected, or hospitalized population are also incorporated. The Hamiltonian and Lagrangian approach is used to derive optimal control law that minimizes the number of infected and the density of contamination of the surfaces. The optimal control law suggested a constant control of $u_1(t) = 1$ and $u_2(t) = u_3(t) = u_4(t) = 0.9$ to bring down the number of infections. Similar optimal control solutions are reported in Kantner and Koprucki [57], Khatua et al. [61], Mandal et al. [80], Tsay et al. [124].

A few literature items report mitigation protocols for COVID-19 by explicitly accounting for time delay involved in disease transmission dynamics in the model [12,32,79,106]. In [12], incubation and testing delays are taken into consideration while deriving an optimal control solution to bound the total number of infections, hospitalizations, and COVID-19 related death, at national and state levels. The fractured landscape of the US is considered to illustrate the use of optimal control methods at the state and nation levels. As a delay of 10 days is estimated in the observed data and the delayed active control intervention $u(t) = \mathcal{U}(S(t-\tau), I(t-\tau))$ is used in Ames et al. [12]. The model predictive control method is used in Carli et al. [27] to derive effective control solution for the management of COVID-19 in multiple regions in Italy. Instead of a country-wide approach, the epidemiological data and hospital facilities available in each region are used to solve the problem of minimal use of NPIs in a post lockdown period.

Robust closed-loop control technique such as sliding mode control are also used to investigate mitigation strategies for COVID-19 [93,109]. In [93], a sliding mode-based reference conditioning method is used to derive control law for NPIs towards confining the spread of the pandemic. Specifically, a day by day reduction in the contact rate is suggested to constraint the severely infected so as not to cross ICU capacity. A restriction level index (RLI) is defined in terms of the time duration of restriction and control input (NPI) to quantify and compare various intervention scenarios. Similarly, in Rohith and Devika [109], an adaptive sliding mode control is used to derive control solutions for the containment of COVID-19.

6. Discussion

This pandemic has taught us how important it is to prevent an epidemic than taking it lightly at the beginning and facing the consequence thereafter. There exist many successful containment stories of outbreaks that happened earlier and did not get global media attention just due to the fact that the outbreak did not lead to a pandemic [11,82,111,117,121]. As human behavior is the key factor that decides whether an outbreak will be contained or lead to a pandemic, it is important to create awareness about the effective containment strategies. As the frequency of pandemics is

increasing, observing a world epidemic awareness day or week to campaign the importance of awareness and preparedness among the public may help the generations to come. Awareness generally allows a community to restore their freedom by choosing the solutions for a problem than focusing on the restrictions that limit them. Hence, the successful containment of earlier epidemics should be analyzed further and should be showcased as examples to instill the importance of preparedness and early strategic containment efforts [11,82,111,117,121].

Epidemic modeling involves uniformity assumptions leading to aggregate modeling with uniform compartments. There can be homogenous or heterogeneous interaction of the population in the infected compartment with that of the susceptible compartments. As shown in the previous sections, adding additional compartments to account for social and behavioral aspects address the heterogenous interaction issue to a certain extent [31,129]. Network-based models are also desirable as they allow the analysis of scenarios such as what happens when a node or a link is removed, or to determine removing which node or link in a network allows optimal and cost-effective containment [101].

Existing model-based analysis unanimously suggests that mathematical models are critical tools in facilitating epidemic control and hence, need to be adapted and improved with model parameters that specifically account for social contact, human mobility, economic impact, molecular/genetic aspects of the disease, etc. [38,84]. For instance, the development of a cross-scale model that includes population dynamics, pathogen dynamics in the host, viral shedding, social behavior, and environmental spread is desirable. Studies also highlight that disease transmission rates highly depends on population behavior, and not on population size. Incorporation of time lag involved in testing reporting, information on pathogen load which can be quantified by qRT-PCR (quantified RT-PCR) to discriminate between super spreaders and others are also desirable [31,129]. There can be two kinds of spreaders based on public interaction/individual behavior and based on viral load.

Extensive digital technologies have been utilized in the fight against COVID-19 for case identification, contact tracing, and for various intervention-response evaluations [21]. For instance, in Qatar, along with infrared temperature scanners, a mobile app is used to screen every incoming visitors to the supermarkets, banks, and other public and private organizations. Thus limiting entry to such places only to non-exposed individuals. The existence of completely digitized population data and health data before the pandemic has enabled Qatar to quickly integrate COVID-19 testing and reporting via the public health system and link the test results to each individual's mobile phone. This facilitates the practical implementation and successful deployment of appropriate public health response against disease spread. Apart from the use of control strategies for deriving active intervention protocols, artificial intelligence, and digital methods are used worldwide in many application such as symptom detectors, X-ray image analysis, AI-based intelligent robot assistance for sanitizing, lifting or transporting infected peoples, lockdown patrol, human activity or interaction detection, hospital triage, blood-sample collection, to name some [40,46,86,105,107]. However, AI-based techniques for deriving effective control measures for mitigating the spread is scarce [96]. In [96], a Q-learning-based model-free closed-loop controller that accounts for cost and hospital saturation constraints related to COVID-19 mitigation is discussed.

Challenges pertaining to mathematical model-based research include translation and implementation of the mathematically motivated decision in practice to curtail the spread of COVID-19 or any future pandemic. It is important to conduct post-pandemic validation of mathematical models to re-validate the reliability scale of the models and to increase the confidence of the public, policymakers, and government on mathematical models. Compared to other areas that rely on the model-based study, such as robotics, aeronautics, drug administration, etc., the main challenge in modeling an emerging pandemic is the limited data and knowledge about the transmission parameters and the time scales of intervention-response curves. Conducting post-pandemic model re-validation and analysis is essential to set protocols for tackling future pandemics. Some of the questions that are yet to be answered are: Why the disease severity is widely different age-wise and countrywide? What is the duration of protection expected from vaccines? Can a vaccine developed for the SARS-COV virus can ward off other virus variants effectively? Is there any difference in vaccine efficacy in different age groups? [38,102,123].

7. Conclusion

A concise and unified review of various mathematical models that can be used for scenario-specific analysis and decision making is presented in this paper. Challenges involved and scope for future work in the area of mathematical modeling are also discussed. In general, the positive changes that happened in the health care network and public health response departments should be analyzed and all favorable adaptation that happened as a response to the COVID-19 pandemic should be reinforced towards developing a resilient health care system and prepared public capable of facing future pandemics.

Declaration of Competing Interest

The authors declare that they have no conflict of interest.

Supplementary material

Supplementary material associated with this article can be found, in the online version, at doi:10.1016/j.cmpb.2021.106301

CRediT authorship contribution statement

Regina Padmanabhan: Writing – original draft. **Hadeel S. Abed:** Writing – original draft. **Nader Meskin:** Conceptualization, Writing – review & editing. **Tamer Khattab:** Conceptualization, Writing – review & editing. **Mujahed Shraim:** Writing – review & editing. **Mohammed Abdulla Al-Hitmi:** Writing – review & editing.

References

[1] COVID-19 effective reproductive number (Rt) analysis 28 October, 2020, 2020a, https://ais.paho.org/phip/viz/COVID19Rt.asp.
[2] Rt COVID-19 effective reproductive number (Rt) analysis 1st November, 2020, 2020b, http://epidemicforecasting.org/country-rt-estimates?region=US.
[3] Rt COVID-19 effective reproductive number (Rt) analysis 26 November, 2020, 2020, https://rt.live/.
[4] Transmission of SARS-CoV-2: implications for infection prevention precautions, July, 2020, 2020, https://www.who.int/news-room/commentaries/detail/transmission-of-sars-cov-2-implications-for-infection-prevention-precautions.
[5] L.J. Abu-Raddad, H. Chemaitelly, H.H. Ayoub, Z. Al Kanaani, A. Al Khal, E. Al Kuwari, A.A. Butt, P. Coyle, A. Jeremijenko, A.H. Kaleeckal, et al., Assessment of the risk of SARS-CoV-2 reinfection in an intense re-exposure setting, MedRxiv (2020a).
[6] L.J. Abu-Raddad, H. Chemaitelly, H.H. Ayoub, Z. Al Kanaani, A. Al Khal, E. Al Kuwari, A.A. Butt, P. Coyle, A.N. Latif, R.C. Owen, et al., Characterizing the Qatar advanced-phase SARS-CoV-2 epidemic, MedRxiv (2020b).
[7] S. Alonso-Quesada, M. De la Sen, R. Agarwal, A. Ibeas, An observer-based vaccination control law for an SEIR epidemic model based on feedback linearization techniques for nonlinear systems, Adv. Differ. Equ. 2012 (1) (2012) 161.
[8] S. Alonso-Quesada, M. de la Sen, A. Ibeas, A vaccination control law based on feedback linearization techniques for SEIR epidemic models., in: Bioinformatics, 2012, pp. 76–85.
[9] S. Alonso-Quesada, M. De la Sen, A. Ibeas, A vaccination strategy based on a state feedback control law for linearizing SEIR epidemic models, in: International Joint Conference on Biomedical Engineering Systems and Technologies, Springer, 2012, pp. 195–209.

[10] S. Alonso-Quesada, M. De la Sen, A. Ibeas, R. Nistal, A vaccination strategy based on linearization control techniques for fighting against epidemic diseases propagation, Adv. Differ. Equ. 2013 (1) (2013) 364.
[11] C.L. Althaus, N. Low, E.O. Musa, F. Shuaib, S. Gsteiger, Ebola virus disease outbreak in Nigeria: transmission dynamics and rapid control, Epidemics 11 (2015) 80–84.
[12] A.D. Ames, T.G. Molnár, A.W. Singletary, G. Orosz, Safety-critical control of active interventions for COVID-19 mitigation, IEEE Access 8 (2020) 188454–188474.
[13] R.M. Anderson, C. Vegvari, J. Truscott, B.S. Collyer, Challenges in creating herd immunity to SARS-CoV-2 infection by mass vaccination, Lancet 396 (10263) (2020) 1614–1616.
[14] O.M. Araz, T. Lant, J.W. Fowler, M. Jehn, Simulation modeling for pandemic decision making: acase study with bi-criteria analysis on school closures, Decis. Support Syst. 55 (2) (2013) 564–575.
[15] R. Augustine, S. Das, A. Hasan, S. Abdul Salam, P. Augustine, Y.B. Dalvi, R. Varghese, R. Primavera, H.M. Yassine, A.S. Thakor, et al., Rapid antibody-based COVID-19 mass surveillance: relevance, challenges, and prospects in a pandemic and post-pandemic world, J. Clin. Med. 9 (10) (2020) 3372.
[16] G. Bärwolff, Mathematical modeling and simulation of the COVID-19 pandemic, Systems 8 (3) (2020) 24.
[17] P.M. Beldomenico, Do superspreaders generate new superspreaders? Ahypothesis to explain the propagation pattern of COVID-19, Int. J. Infect. Dis. 96 (2020) 461–463.
[18] G. Benrhmach, K. Namir, J. Bouyaghroumni, Modelling and simulating the novel coronavirus with implications of asymptomatic carriers, Int. J. Differ. Equ. (2020) 5487147.
[19] S. Bhumbra, S. Malin, L. Kirkpatrick, A. Khaitan, C.C. John, C.M. Rowan, L.A. Enane, Clinical features of critical coronavirus disease 2019 in children, Pediatr. Crit. Care Med. 21 (10) (2020) e948.
[20] T. Britton, F. Ball, P. Trapman, A mathematical model reveals the influence of population heterogeneity on herd immunity to SARS-CoV-2, Science 369 (6505) (2020) 846–849.
[21] J. Budd, B.S. Miller, E.M. Manning, V. Lampos, M. Zhuang, M. Edelstein, G. Rees, V.C. Emery, M.M. Stevens, N. Keegan, et al., Digital technologies in the public-health response to COVID-19, Nat. Med. 26 (8) (2020) 1183–1192.
[22] C.A.H. Buhat, M.C. Torres, Y.H. Olave, M.K.A. Gavina, E.F.O. Felix, G.B. Gamilla, K.V.B. Verano, A.L. Babierra, J.F. Rabajante, A mathematical model of COVID-19 transmission between frontliners and the general public, MedRxiv (2020).
[23] C. Bulut, Y. Kato, Epidemiology of COVID-19, Turk. J. Med. Sci. 50 (SI-1) (2020) 563–570.
[24] B. Buonomo, Effects of information-dependent vaccination behavior on coronavirus outbreak:iinsights from a SIRI model, Ric. Mat. 69 (2) (2020) 483–499.
[25] D. Buonsenso, D. Roland, C. De Rose, P. Vásquez-Hoyos, B. Ramly, J.N. Chakakala-Chaziya, A. Munro, S. González-Dambrauskas, Schools closures during the COVID-19 pandemic: a catastrophic global situation (2020).
[26] T.K. Burki, The russian vaccine for COVID-19, Lancet Respir. Med. 8 (11) (2020) e85–e86.
[27] R. Carli, G. Cavone, N. Epicoco, P. Scarabaggio, M. Dotoli, Model predictive control to mitigate the COVID-19 outbreak in a multi-region scenario, Annu. Rev. Control 50 (2020) 373–393.
[28] C. Carroll, S. Bhattacharjee, Y. Chen, P. Dubey, J. Fan, A. Gajardo, X. Zhou, H.-G. Müller, J.-L. Wang, Time dynamics of COVID-19, Sci. Rep. 10 (1) (2020) 1–14.
[29] A.K. Chan, C. Nickson, J. Rudolph, A. Lee, G. Joynt, Social media for rapid knowledge dissemination: early experience from the COVID-19 pandemic, Wiley Online Library 75 (2020) 1579–1582.
[30] J.Y. Chao, K.R. Derespina, B.C. Herold, D.L. Goldman, M. Aldrich, J. Weingarten, H.M. Ushay, M.D. Cabana, S.S. Medar, Clinical characteristics and outcomes of hospitalized and critically ill children and adolescents with coronavirus disease 2019 (COVID-19) at a tertiary care medical center in new york city, J. Pediatr. 223 (2020) 14–19.
[31] S. Chen, P. Robinson, D. Janies, M. Dulin, Four challenges associated with current mathematical modeling paradigm of infectious diseases and call for a shift, in: Open forum Infectious Diseases, 7, Oxford University Press US, 2020, p. ofaa333.
[32] Y. Chen, J. Cheng, Y. Jiang, K. Liu, A time delay dynamical model for outbreak of 2019-nCoV and the parameter identification, J. Inverse Ill-Posed Probl. 28 (2) (2020) 243–250.
[33] N.G. Davies, P. Klepac, Y. Liu, K. Prem, M. Jit, R.M. Eggo, Age-dependent effects in the transmission and control of COVID-19 epidemics, Nat. Med. 26 (8) (2020) 1205–1211.
[34] R. Djidjou-Demasse, Y. Michalakis, M. Choisy, M.T. Sofonea, S. Alizon, Optimal COVID-19 epidemic control until vaccine deployment, medRxiv (2020).
[35] A.A. Dror, N. Eisenbach, S. Taiber, N.G. Morozov, M. Mizrachi, A. Zigron, S. Srouji, E. Sela, Vaccine hesitancy: the next challenge in the fight against COVID-19, Eur. J. Epidemiol. 35 (8) (2020) 775–779.
[36] S.Q. Du, W. Yuan, Mathematical modeling of interaction between innate and adaptive immune responses in COVID-19 and implications for viral pathogenesis, J. Med. Virol. 92 (9) (2020) 1615–1628.
[37] N.M. Duggan, S.M. Ludy, B.C. Shannon, A.T. Reisner, S.R. Wilcox, Is novel coronavirus 2019 reinfection possible? Interpreting dynamic SARS-CoV-2 test results through a case report, Am. J. Emerg. Med. 39 (2020) 256–e1.
[38] F.C. Fang, C.A. Benson, C. Del Rio, K.M. Edwards, V.G. Fowler Jr, D.N. Fredricks, A.P. Limaye, B.E. Murray, S. Naggie, P.G. Pappas, et al., COVID-19–lessons learned and questions remaining, Clin. Infect. Dis. 72 (2020) 2225–2240.
[39] E.S. Fonfria, M.I. Vigo, D. García-García, Z. Herrador, M. Navarro, C. Bordehore, Essential epidemiological parameters of COVID-19 for clinical and mathematical modeling purposes: a rapid review and meta-analysis, MedRxiv (2020).
[40] S.J. Fong, N. Dey, J. Chaki, Artificial Intelligence for Coronavirus Outbreak, Springer, 2020.
[41] E. Forgoston, M. Thorne, Strategies for controlling the spread of COVID-19, MedRxiv (2020).
[42] M. Garcia-Cremades, B.P. Solans, E. Hughes, J.P. Ernest, E. Wallender, F. Aweeka, A.F. Luetkemeyer, R.M. Savic, Optimizing hydroxychloroquine dosing for patients with COVID-19: an integrative modeling approach for effective drug repurposing, Clin. Pharmacol. Ther. 108 (2) (2020) 253–263.
[43] G. Giordano, F. Blanchini, R. Bruno, P. Colaneri, A. Di Filippo, A. Di Matteo, M. Colaneri, Modelling the COVID-19 epidemic and implementation of population-wide interventions in italy, Nat. Med. 26 (2020) 1–6.
[44] M. Gousseff, P. Penot, L. Gallay, D. Batisse, N. Benech, K. Bouiller, R. Collarino, A. Conrad, D. Slama, C. Joseph, et al., Clinical recurrences of COVID-19 symptoms after recovery: viral relapse, reinfection or inflammatory rebound? J. Infect. 81 (5) (2020) 816–846.
[45] T. Guardian, School closures could wipe 3% from uk GDP, ministers warned (2020). https://www.theguardian.com/education/2020/mar/13/coronavirus-school-closures-uk-gdp-ministers-warned.
[46] N. Haug, L. Geyrhofer, A. Londei, E. Dervic, A. Desvars-Larrive, V. Loreto, B. Pinior, S. Thurner, P. Klimek, Ranking the effectiveness of worldwide COVID-19 government interventions, Nat. Hum. Behav. 4 (12) (2020) 1303–1312.
[47] H. He, Y. Shen, C. Jiang, T. Li, M. Guo, L. Yao, Spatiotemporal big data for PM2.5 exposure and health risk assessment during COVID-19, Int. J. Environ. Res. Public Health 17 (20) (2020) 7664.
[48] J. Hellewell, S. Abbott, A. Gimma, N.I. Bosse, C.I. Jarvis, T.W. Russell, J.D. Munday, A.J. Kucharski, W.J. Edmunds, F. Sun, et al., Feasibility of controlling COVID-19 outbreaks by isolation of cases and contacts, Lancet Global Health 8 (2020) e488–e496.
[49] E.A. Hernandez-Vargas, J.X. Velasco-Hernandez, In-host mathematical modelling of COVID-19 in humans, Annu. Rev. Control 50 (2020) 448–456.
[50] W. Hu, Y. Shi, Z. Chen, Optimal pandemic control: limited resource and human mobility, Available at SSRN 3660315 (2020).
[51] M.A. Ibrahim, A. Al-Najafi, Modeling, control, and prediction of the spread of COVID-19 using compartmental, logistic, and gauss models: a case study in Rraq and Egypt, Processes 8 (11) (2020) 1400.
[52] A. Iwasaki, What reinfections mean for COVID-19, Lancet Infect. Dis. 21 (1) (2020) 35.
[53] C. Jackson, P. Mangtani, J. Hawker, B. Olowokure, E. Vynnycky, The effects of school closures on influenza outbreaks and pandemics: systematic review of simulation studies, PLoS One 9 (5) (2014) e97297.
[54] L. Jiang, K. Tang, M. Levin, O. Irfan, S.K. Morris, K. Wilson, J.D. Klein, Z.A. Bhutta, COVID-19 and multisystem inflammatory syndrome in children and adolescents, Lancet Infect. Dis. 20 (2020) e276–e288.
[55] P. Jiang, X. Fu, Y. Van Fan, J.J. Klemeš, P. Chen, S. Ma, W. Zhang, Spatial-temporal potential exposure risk analytics and urban sustainability impacts related to COVID-19 mitigation: a perspective from car mobility behaviour, J. Clean. Prod. 279 (2020) 123673.
[56] C.-E. Juneau, T. Pueyo, M. Bell, G. Gee, L. Potvin, Evidence-based, cost-effective interventions to suppress the COVID-19 pandemic: a rapid systematic review, Medrxiv (2020).
[57] M. Kantner, T. Koprucki, Beyond just æflattening the curveg: optimal control of epidemics with purely non-pharmaceutical interventions, J. Math. Ind. 10 (1) (2020) 1–23.
[58] V. Karatayev, M. Anand, C.T. Bauch, The far side of the COVID-19 epidemic curve: local re-openings based on globally coordinated triggers may work best, medRxiv (2020).
[59] S.M. Kassa, J.B. Njagarah, Y.A. Terefe, Analysis of the mitigation strategies for COVID-19: from mathematical modelling perspective, Chaos Solitons Fractals 138 (2020) 109968.
[60] S. Kaushik, S.I. Aydin, K.R. Derespina, P.B. Bansal, S. Kowalsky, R. Trachtman, J.K. Gillen, M.M. Perez, S.H. Soshnick, E.E. Conway Jr, et al., Multisystem inflammatory syndrome in children associated with severe acute respiratory syndrome coronavirus 2 infection: a multi-institutional study from New York city, J. Pediatr. 224 (2020) 24–29.
[61] D. Khatua, A. De, S. Kar, E. Samanta, S.M. Mandal, A dynamic optimal control model for SARS-CoV-2 in India, Available at SSRN 3597498 (2020).
[62] S. Kim, Y.-J. Kim, K.R. Peck, E. Jung, School opening delay effect on transmission dynamics of coronavirus disease 2019 in Korea: based on mathematical modeling and simulation study, J. Korean Med. Sci. 35 (13) (2020).
[63] A. Kotwal, A.K. Yadav, J. Yadav, J. Kotwal, S. Khune, Predictive models of COVID-19 in India: a rapid review, Med. J. Armed Forces India 76 (4) (2020) 377–386.
[64] Y. Kouakep, S. Tchoumi, D. Fotsa, F. Kamba, D. Ngounou, E. Mboula, V. Kamla, J. Kamgang, Modelling the anti-COVID-19 individual or collective containment strategies in cameroon, Appl. Math. Sci. 15 (2) (2021) 63–78.
[65] A.J. Kucharski, T.W. Russell, C. Diamond, Y. Liu, J. Edmunds, S. Funk, R.M. Eggo, F. Sun, M. Jit, J.D. Munday, et al., Early dynamics of transmission and control of COVID-19: a mathematical modelling study, Lancet Infect. Dis. 20 (5) (2020) 553–558.

[66] V. Kumar, A. Sood, S. Gupta, N. Sood, Prevention-versus promotion-focus regulatory efforts on the disease incidence and mortality of COVID-19: amultinational diffusion study using functional data analysis, J. Int. Mark. 29 (2020) 1–22. 1069031X20966563
[67] L. Laguzet, G. Turinici, Globally optimal vaccination policies in the SIR model: smoothness of the value function and uniqueness of the optimal strategies, Math. Biosci. 263 (2014) 180–197.
[68] A. Lahiri, S.S. Jha, S. Bhattacharya, S. Ray, A. Chakraborty, et al., Effectiveness of preventive measures againstCOVID-19: a systematic review of in silico modeling studies in indian context, Indian J. Public Health 64 (6) (2020) 156.
[69] H. Lempel, J.M. Epstein, R.A. Hammond, Economic cost and health care workforce effects of school closures in the US, PLoS Curr. 1 (2009) PMC2762813.
[70] D. Lewis, Mounting evidence suggests coronavirus is airbornebut health advice has not caught up, Nature 583 (7817) (2020) 510–513.
[71] R. Li, S. Pei, B. Chen, Y. Song, T. Zhang, W. Yang, J. Shaman, Substantial undocumented infection facilitates the rapid dissemination of novel coronavirus (SARS-CoV-2), Science 368 (6490) (2020) 489–493.
[72] Y.-F. Lin, Q. Duan, Y. Zhou, T. Yuan, P. Li, T. Fitzpatrick, L. Fu, A. Feng, G. Luo, Y. Zhan, et al., Spread and impact of COVID-19 in China: a systematic review and synthesis of predictions from transmission-dynamic models, Front. Med. 7 (2020) 321.
[73] Z. Liu, P. Magal, O. Seydi, G. Webb, A COVID-19 epidemic model with latency period, Infect. Dis. Model. 5 (2020) 323–337.
[74] L.C. Lopes-Júnior, E. Bomfim, D.S.C. da Silveira, R.M. Pessanha, S.I.P.C. Schuab, R.A.G. Lima, Effectiveness of mass testing for control of COVID-19: a systematic review protocol, BMJ Open 10 (8) (2020) e040413.
[75] J. Ma, Estimating epidemic exponential growth rate and basic reproduction number, Infect. Dis. Model. 5 (2020) 129–141.
[76] C.E. Madubueze, D. Sambo, I.O. Onwubuya, Controlling the spread of COVID-19: optimal control analysis, MedRxiv (2020).
[77] E. Mahase, COVID-19: Pfizer and BioNTech submit vaccine for US authorisation, 2020.
[78] M. Makhoul, H.H. Ayoub, H. Chemaitelly, S. Seedat, G.R. Mumtaz, S. Al-Omari, L.J. Abu-Raddad, Epidemiological impact of SARS-CoV-2 vaccination: mathematical modeling analyses, Vaccines 8 (4) (2020) 668.
[79] M. Maleewong, Time delay epidemic model for COVID-19, MedRxiv (2020).
[80] M. Mandal, S. Jana, S.K. Nandi, A. Khatua, S. Adak, T. Kar, A model based study on the dynamics of COVID-19: prediction and control, Chaos Solitons Fractals 136 (2020) 109889.
[81] L. Matrajt, J. Eaton, T. Leung, E.R. Brown, Vaccine optimization for COVID-19, who to vaccinate first?, MedRxiv (2020).
[82] A.K. Mbonye, J.F. Wamala, M. Nanyunja, A. Opio, I. Makumbi, J.R. Aceng, Ebola viral hemorrhagic disease outbreak in West Africa-lessons from Uganda., Afr. Health Sci. 14 (3) (2014) 495–501.
[83] C. McAloon, Á. Collins, K. Hunt, A. Barber, A.W. Byrne, F. Butler, M. Casey, J. Griffin, E. Lane, D. McEvoy, et al., Incubation period of COVID-19: a rapid systematic review and meta-analysis of observational research, BMJ Open 10 (8) (2020) e039652.
[84] E.S. McBryde, M.T. Meehan, O.A. Adegboye, A.I. Adekunle, J.M. Caldwell, A. Pak, D.P. Rojas, B. Williams, J.M. Trauer, Role of modelling in COVID-19 policy development, Paediatr. Respir. Rev. 35 (2020) 57–60.
[85] M.T. Meehan, D.P. Rojas, A.I. Adekunle, O.A. Adegboye, J.M. Caldwell, E. Turek, B. Williams, J.M. Trauer, E.S. McBryde, Modelling insights into the COVID-19 pandemic, Paediatr. Respir. Rev. 35 (2020) 64–69.
[86] P. Melin, J.C. Monica, D. Sanchez, O. Castillo, Multiple ensemble neural network models with fuzzy response aggregation for predicting COVID-19 time series: the case of Mexico, in: Healthcare, 8, Multidisciplinary Digital Publishing Institute, 2020, p. 181.
[87] K. Mizumoto, R. Omori, H. Nishiura, Age specificity of cases and attack rate of novel coronavirus disease (COVID-19), MedRxiv (2020).
[88] C. Modchang, S. Iamsirithaworn, P. Auewarakul, W. Triampo, A modeling study of school closure to reduce influenza transmission: a case study of an influenza a (h1n1) outbreak in a private thai school, Math. Comput. Model. 55 (3–4) (2012) 1021–1033.
[89] Y. Mohamadou, A. Halidou, P.T. Kapen, A review of mathematical modeling, artificial intelligence and datasets used in the study, prediction and management of COVID-19, Appl. Intell. 50 (2020) 3913–3925.
[90] A.A. Momoh, A. Fugenschuh, Optimal control of intervention strategies and cost effectiveness analysis for a Zika virus model, Oper. Res. Health Care 18 (2018) 99–111.
[91] Z. Mukandavire, F. Nyabadza, N.J. Malunguza, D.F. Cuadros, T. Shiri, G. Musuka, Quantifying early COVID-19 outbreak transmission in South Africa and exploring vaccine efficacy scenarios, PLoS One 15 (7) (2020) e0236003.
[92] G. Mumtaz, H. Ayoub, M. Makhoul, S. Seedat, H. Chemaitelly, L. Abu-Raddad, Can the COVID-19 pandemic still be suppressed? putting essential pieces together, J. Global Health Rep. 4 (2020) e2020030.
[93] S. Nuñez, F.A. Inthamoussou, F. Valenciaga, H. De Battista, F. Garelli, Potentials of constrained sliding mode control as an intervention guide to manage COVID-19 spread, MedRxiv (2020).
[94] J.F. Oliveira, D.C. Jorge, R.V. Veiga, M.S. Rodrigues, M.F. Torquato, N.B. da Silva, R.L. Fiaccone, L.L. Cardim, F.A. Pereira, C.P. de Castro, et al., Mathematical modeling of COVID-19 in 14.8 million individuals in Bahia, Brazil, Nat. Commun. 12 (1) (2020) 1–13.
[95] M. Ota, Will we see protection or reinfection in COVID-19? Nat. Rev. Immunol. 20 (6) (2020) 351.
[96] R. Padmanabhan, N. Meskin, T. Khattab, M. Shraim, M. Al-Hitmi, Reinforcement learning-based decision support system for COVID-19, Biomed. Signal Process. Control 68 (2021) 102676.
[97] M. Park, A.R. Cook, J.T. Lim, Y. Sun, B.L. Dickens, A systematic review of COVID-19 epidemiology based on current evidence, J. Clin. Med. 9 (4) (2020) 967.
[98] R.W. Paterson, R.L. Brown, L. Benjamin, R. Nortley, S. Wiethoff, T. Bharucha, D.L. Jayaseelan, G. Kumar, R.E. Raftopoulos, L. Zambreanu, et al., The emerging spectrum of COVID-19 neurology: clinical, radiological and laboratory findings, Brain 143 (10) (2020) 3104–3120.
[99] L. Peng, W. Yang, D. Zhang, C. Zhuge, L. Hong, Epidemic analysis of COVID-19 in China by dynamical modeling, ArXiv Preprint arXiv:2002.06563 (2020).
[100] B. Phillips, D. Browne, M. Anand, C. Bauch, Model-based projections for COVID-19 outbreak size and student-days lost to closure in Ontario childcare centres and primary schools, MedRxiv (2020).
[101] A.T. Porter, J.J. Oleson, A path-specific SEIR model for use with general latent and infectious time distributions, Biometrics 69 (1) (2013) 101–108.
[102] K. Prem, Y. Liu, T.W. Russell, A.J. Kucharski, R.M. Eggo, N. Davies, S. Flasche, S. Clifford, C.A. Pearson, J.D. Munday, et al., The effect of control strategies to reduce social mixing on outcomes of the COVID-19 epidemic in Wuhan, China: a modelling study, Lancet Public Health 5 (5) (2020) e261–e270.
[103] J.F. Rabajante, Insights from early mathematical models of 2019-nCoV acute respiratory disease (COVID-19) dynamics, arXiv preprint arXiv:2002.05296 (2020).
[104] N. Rajapakse, D. Dixit, Human and novel coronavirus infections in children: a review, Paediatr. Int. Child Health (2020) 1–20.
[105] A.S.S. Rao, J.A. Vazquez, Identification of COVID-19 can be quicker through artificial intelligence framework using a mobile phone–based survey when cities and towns are under quarantine, Infect. Control Hosp. Epidemiol. 41 (7) (2020) 826–830.
[106] M. Rasha, S. Balamuralitharan, A study on COVID-19 transmission dynamics: stability analysis of SEIR model with Hopf bifurcation for effect of time delay, Adv. Differ. Equ. 2020 (1) (2020) 1–20.
[107] K. Raza, Artificial intelligence against COVID-19: a meta-analysis of current research, in: Big Data Analytics and Artificial Intelligence Against COVID-19: Innovation Vision and Approach, 2020, pp. 165–176.
[108] A. Robert, Lessons from new zealand's COVID-19 outbreak response, Lancet Public Health 5 (11) (2020) e569–e570.
[109] G. Rohith, K. Devika, Dynamics and control of COVID-19 pandemic with nonlinear incidence rates, Nonlinear Dyn. 101 (3) (2020) 2013–2026.
[110] M.Z. Sadique, E.J. Adams, W.J. Edmunds, Estimating the costs of school closure for mitigating an influenza pandemic, BMC Public Health 8 (1) (2008) 135.
[111] R.R. Sahay, P.D. Yadav, N. Gupta, A.M. Shete, C. Radhakrishnan, G. Mohan, N. Menon, T. Bhatnagar, K. Suma, A.V. Kadam, et al., Experiential learnings from the Nipah virus outbreaks in Kerala towards containment of infectious public health emergencies in India, Epidemiol. Infect. 148 (2020).
[112] A. Scherer, A. McLean, Mathematical models of vaccination, Br. Med. Bull. 62 (1) (2002) 187–199.
[113] M. De la Sen, S. Alonso-Quesada, A simple vaccination control strategy for the SEIR epidemic model, in: 2010 IEEE International Conference on Management of Innovation & Technology, IEEE, 2010, pp. 1037–1044.
[114] K. Shah, A. Awasthi, B. Modi, R. Kundapur, D.B. Saxena, Unfolding trends of COVID-19 transmission in India: critical review of available mathematical models., Indian J. Community Health 32 (2) (2020) 206–214.
[115] M. Sharifi, H. Moradi, Nonlinear robust adaptive sliding mode control of influenza epidemic in the presence of uncertainty, J. Process Control 56 (2017) 48–57.
[116] M. Shen, Z. Peng, Y. Xiao, L. Zhang, Modeling the epidemic trend of the 2019 novel coronavirus outbreak in China, Innovation 1 (3) (2020) 100048.
[117] V. Soman Pillai, G. Krishna, M. Valiya Veettil, Nipah virus: past outbreaks and future containment, Viruses 12 (4) (2020) 465.
[118] A. Srivastava, G. Chowell, Understanding spatial heterogeneity of COVID-19 pandemic using shape analysis of growth rate curves, medRxiv (2020).
[119] G. Stewart, K. Heusden, G.A. Dumont, How control theory can help us control COVID-19, IEEE Spectr. 57 (6) (2020) 22–29.
[120] H. Swapnarekha, H.S. Behera, J. Nayak, B. Naik, Role of intelligent computing in COVID-19 prognosis: a state-of-the-art review, Chaos Solitons Fractals 138 (2020) 109947.
[121] C.-C. Tan, SARS in Singapore-key lessons from an epidemic, Ann. Acad. Med. Singapore 35 (5) (2006) 345.
[122] G.S.E. Tan, A. Hou, C.M. Manauis, J.M. Chua, C.Q. Gao, F.K.K. Ng, C.S. Wong, O.-T. Ng, K. Marimuthu, M. Chan, et al., Reducing hospital admissions for COVID-19 at a dedicated screening centre in singapore, Clin. Microbiol. Infect. 26 (9) (2020) 1278–1279.
[123] L. Tang, Y. Zhou, L. Wang, S. Purkayastha, L. Zhang, J. He, F. Wang, P.X.-K. Song, A review of multi-compartment infectious disease models, Int. Stat. Rev. 88 (2) (2020) 462–513.
[124] C. Tsay, F. Lejarza, M.A. Stadtherr, M. Baldea, Modeling, state estimation, and optimal control for the US COVID-19 outbreak, arXiv preprint arXiv:2004.06291 (2020).
[125] J.H. university, medicine, Recent opening and closing policy decisions(2020). https://coronavirus.jhu.edu/data/state-timeline/new-confirmed-cases/hawaii.
[126] R. Vaishya, M. Javaid, I.H. Khan, A. Haleem, Artificial intelligence (AI) applications for COVID-19 pandemic, Diabetes Metab. Syndr. (2020).

[127] R. Verma, Fuzzy modeling for the spread of influenza virus and its possible control, Comput. Ecol. Softw. 8 (2018) 32–45.
[128] A. Victor, Mathematical predictions for COVID-19 as a global pandemic, Available at SSRN 3555879 (2020).
[129] J. Wang, Mathematical models for COVID-19: applications, limitations, and potentials, J. Public Health Emerg. 4 (2020).
[130] N. Wang, Y. Fu, H. Zhang, H. Shi, An evaluation of mathematical models for the outbreak of COVID-19, Precis. Clin. Med. 3 (2) (2020) 85–93.
[131] W. Wang, Backward bifurcation of an epidemic model with treatment, Math. Biosci. 201 (1–2) (2006) 58–71.
[132] X. Wang, M. Shen, Y. Xiao, L. Rong, Optimal control and cost-effectiveness analysis of a Zika virus infection model with comprehensive interventions, Appl. Math. Comput. 359 (2019) 165–185.
[133] WHO, Anticipating emerging infectious disease epidemics(2016). https://apps.who.int/iris/bitstream/handle/10665/252646/WHO-OHE-PED-2016.2-eng.pdf.
[134] P. Yang, X. Wang, COVID-19: a new challenge for human beings, Cell. Mol. Immunol. 17 (5) (2020) 555–557.
[135] M. Zamir, Z. Shah, F. Nadeem, A. Memood, H. Alrabaiah, P. Kumam, Non pharmaceutical interventions for optimal control of COVID-19, Comput. Methods Prog. Biomed. 196 (2020) 105642.